1.1 Introduction

Nowadays, in the field of semiconductor technology, the most productive research area is organic electronics which includes both conducting small molecules like pentacene as well as polymeric molecules. Rather than small molecules, we concentrated our work on polymeric molecules based charge transport properties, as this area is highly fascinating in terms of low-cost electronics. Since the conventional inorganic electronics are frequently produced by applying the complex and absolutely expensive processing techniques demanding equally high-class clean room facilities along with sophisticated vacuum equipment, one of the extremely desirable attributes with organic materials is that they can be processed from solution [Forrest (2004), Facchetti (2010), Sekitani and Someya (2010)]. This empowers numerous inexpensive manufacturing techniques, in precisely the same way as ink is deposited on paper, and starts up the possibility to utilize non-traditional substrates, such as for example flexible plastic, foils, paper and also the cloths [Forrest (2004), Borchardt (2004), Allen (2005), Hamedi et al. (2007), Facchetti and Marks (2010), Zhuang et al. (2013)]. Therefore, organic electronics is acting as breakthrough for the electronic industries by presenting the flexible and smooth platform [Gaudiana and Brabec (2008), Irimia-Vladu (2014), Ling et al. (2018), Wang et al. (2019)]. This is due to the several advantages over traditional electronics like better flexibility, minimal cost and lighter in weight. Actually in this area, electronic devices grounded on organic materials ensure numerous characteristics that can conquer several significant issues connected with that of inorganic semiconductor [Mitzi et al. (2001), Forrest (2003), Kelley et al. (2004), Sun et al. (2005)]; thus, for the commercial as well as technical applications of high potential, the polymer electronics is now expected to be an emerging section of world-wide scientific research. The comparative properties of inorganic (conventional) *vs.* organic

electronics is tabulated and summarized in Table 1.1 and Fig. 1.1 respectively. However, it is much significant to note here that performance of organic materials cannot compete with single crystal silicon technology in terms of mobility (more than 1000 cm^2/Vs). Since, the performance of amorphous silicon technology, having the mobility in the range ~1cm^2/Vs (comparatively much lesser than that of single crystal silicon) may be competed by that of organic materials especially organic conjugated polymers (OCPs) [Sirringhaus et al. (1998)]. This is due to the unique advantage associated with organic semiconductors (OSCs) as they possess application based synthesis with variation in functionality, where amorphous silicon technology lags [Wang et al. (2012)]. Somehow, the dielectric constant is a key factor to have enhanced properties in conventional inorganic semiconductors. As per the Coulomb's law; $F = (1/4\varepsilon_0\varepsilon_r)\ (q_1q_2/r^2)$, the dielectric constant (ε_r) is directly associated with the excitons (photogenerated electron-hole pairs) size, and the dissociation of excitons is the prime factor for carrier generation in OSCs. This dielectric constant directly correlates the (a) Exciton type, (b) Exciton binding energy, and (c) Exciton radius. For example, the dielectric constant is large in the case of inorganic semiconductors (e.g. for GaAs, ε_r=12.9), causes a larger exciton radius (160 Å) localized on large GaAs atoms (Fig.1.2). This Wannier-type exciton immediately dissociates (due to weaker binding energy; ~5meV) to a free electron and a hole from thermal energy at room temperature and generates photocurrent. On the other hand, organic semiconductors possess small values of the dielectric constant (e.g. for OSC (C_{60}), ε_r=4) causes very small exciton radius (10 Å) localized on a single C_{60} molecule (Fig.1.2). These Frenkel-typeexcitons are hardly dissociated (due to strong binding energy; ~1eV) to free electrons and holes by thermal energy of room temperature. Therefore, OSCs can produce comparatively less photocarriers. This is the reason why the initially fabricated organic solar cells showed

extremely low photocurrents, of the order of nano- to micro-amperes [Hiramoto et al. (2014)].

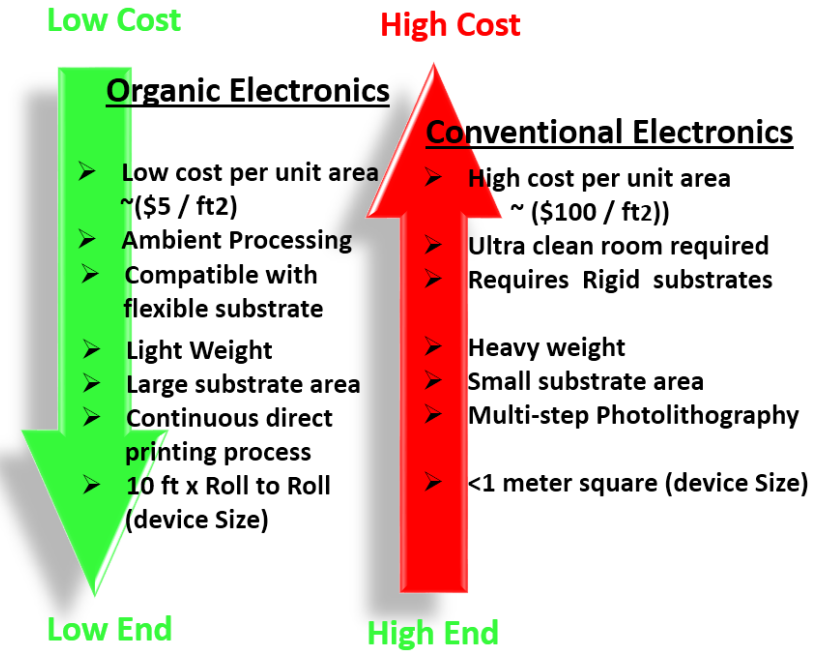

Fig.1.1 Comparative properties of organic *vs.* conventional electronics.

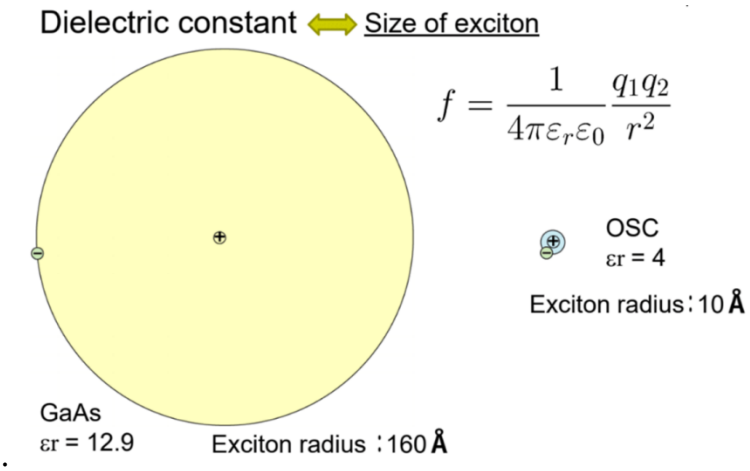

Fig. 1.2 Size of excitons for an inorganic semiconductor and an organic semiconductor [Hiramoto et al. (2014)].

Table: 1.1 General comparison between organic and inorganic semiconductors.

Properties	**Organic Semiconductors**	**Inorganic Semiconductors**
Dielectric Constant (ε_r)	~3.5	~12
Band gap	~50-500 meV.	Several eV.
Crystal basis	Molecules	Atoms
Exciton binding energy	0.5-1 eV	5 meV
Exciton type	Mostly Frankel, Sometimes CT	Wannier
Exciton radius	0.5-1 nm	5-10 nm
Band transport	Below 300K, depends upon crystallographic orientation	Always allowed
Mobility	1-100 cm^2/Vs @300K 100 cm^2/Vs @10K	1000-10000 cm^2/Vs @300K

In conclusion, it is noteworthy that concrete goal of the organic electronics is not to compete with crystalline silicon technology, but to replace amorphous silicon technology through exclusive properties of organic semiconductors in different areas. Nevertheless, the OSCs ensure good flexibility as well as high strength, but normally they possess towards insulating behaviour in fully reduced state. The boost in the development of polymers, possessing the electrical conductivity came into the picture just after the report of Weiss *et al.* in 1963, related to conductivity inside the polypyrrole on doping with iodine, following the discovery of the semiconducting properties of polyacetylene in the 1977 [McNeill et al. (1963), Shirakawa et al. (1977), Chiang et al. (1977)]. As per the report, when polyacetylene was treated with iodine, the conductivity of polyacetylene, an organic polymer was transformed by seven orders of magnitude, leading to conductivity near to being metallic in its identity [Chiang et al. (1977)]. Further for this innovation i.e. 'the discovery development of conductive polymers', Profs. Alan J. Heeger, Alan G. MacDiarmid, & Hideki Shirakawa were awarded jointly with Nobel Prize (Chemistry) in

the year 2000. As discussed earlier; the crucial parameters for using the organic semiconductors are its better solution processability, having excellent electronic properties as well as cost effectiveness. However, the ultimate test of organic semiconductors lies in the reliability, sustainability, and performance of the electronic devices made up of these materials. Although the term 'cost-effectiveness' can be importantly measured by the factor of the overall associated cost. Though the involved materials cost is meager, its fabrication and packaging costs enhance the total cost of device fabrication. Hence, the successful application of organic conducting polymer materials as electronic devices (over the large area substrates) is to produce the cost-effective innovative processing techniques. The leading cause of having the better electronic properties of organic semiconductors in electronics devices is their electronic structure. Because, it's a tedious job to modify the natural properties such as molecular interactions and chemical framework pertaining to the organic materials. Nevertheless, the incorporation of template or directing forces may lead to the possibility to tune assembly which ultimately stimulates their crystallinity and consequently modifies the electronic properties. The improvement of crystallinity of these materials by utilizing their property of self-assembly can be quite a method for improving the electronic properties of such materials. It is well known that through self-organization of organic materials, the materials stability, charge transport, and mobility can be increased several folds within electronic / optoelectronics devices [Yu et al. (2012), Jung et al. (2007)]. It broadens up a plenty of opportunity to enhance the property of materials by proper alignment of polymer chains, the advancement in carrier mobility, stability, crystallinity, etc. [Kushida et al. (2011), Nagamatsu et al. (2003), Ong et al. (2004), Singh and Prakash (2012)].

1.2 Organic conducting polymers

Organic conducting polymer (OCP) is a class of organic polymer that contains π-conjugated system and ability to conduct charges through delocalization or hopping process. It may be acyclic (polyacetylene), carbocyclic (polyphenylene, polyaniline, polyanthranilic acid etc.) and hetrocyclic (polyindole, polythiophene, polypyrrole etc.) as shown in Fig. 1.3.

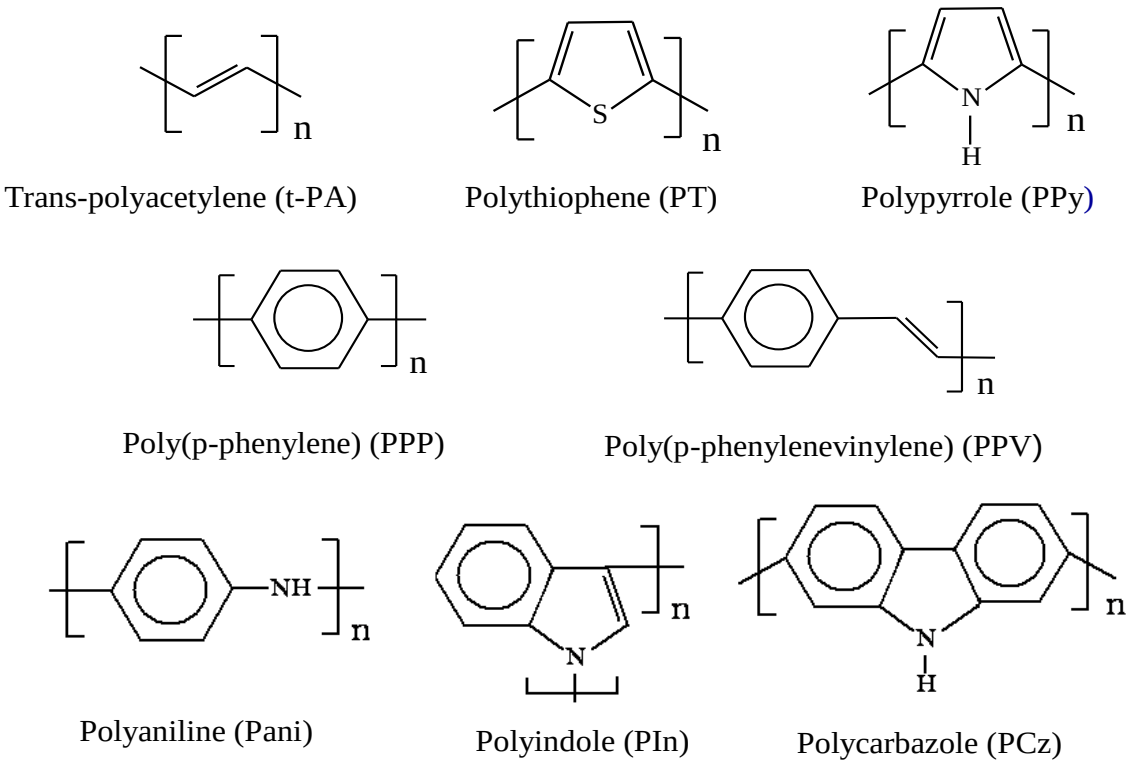

Trans-polyacetylene (t-PA) Polythiophene (PT) Polypyrrole (PPy)

Poly(p-phenylene) (PPP) Poly(p-phenylenevinylene) (PPV)

Polyaniline (Pani) Polyindole (PIn) Polycarbazole (PCz)

Fig. 1.3 Chemical structures of common carbocyclic and heterocyclic organic conducting polymers. Here 'n' written outside the parenthesis represents union of the respective monomers [Ghosh et al. (2016), Singh (2010)].

One thing common herein such family which can be seen that multiple bonds in conjugation state is necessary. In these structures, the formation of σ-bonds (C-C) in the polymer chains takes place as a result of orbitals overlapping (sp^2 hybridized) in xy-plane (molecular plane), whereas the formation of π-bonds (C=C or C=X where X is hetero

atom) takes place as a result of remaining orbitals using side-by-side overlapping (p_z, un-hybridized orbitals) of individual carbon or hetero atom. To understand these things, the sigma-pi model for ethylene and the delocalized π-electron-system in a benzene ring shown in Fig 1.4. Same concept is extended in case of overlapping of carbon with hetero atom (s).

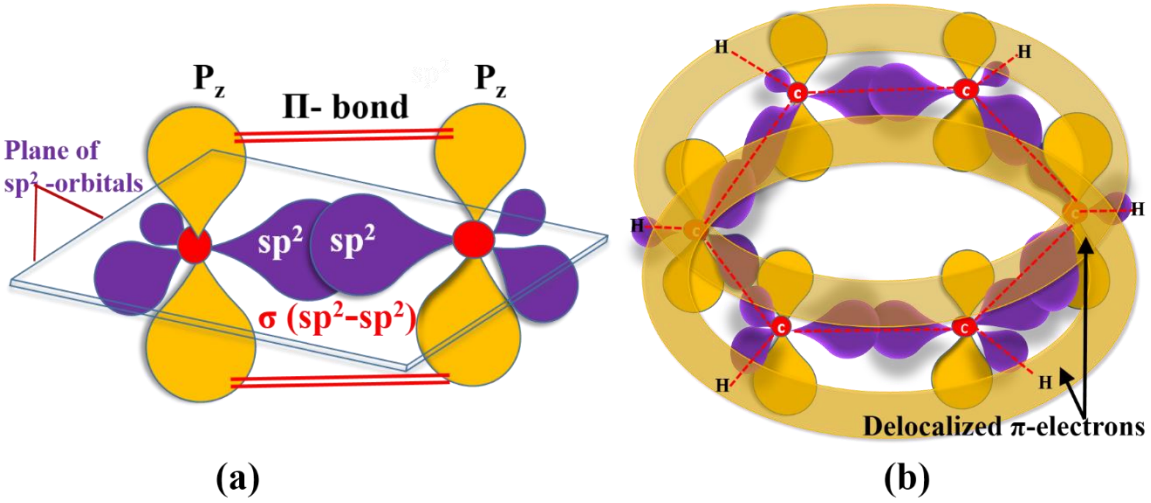

Fig. 1.4 (a) In ethylene, the sigma-pi bonding of carbon atoms, **(b)** In benzene ring, the delocalized π-electron-system.

Those electrons, which are not involved in bond formations, are remains as such as lone pair of electrons. For example, in case of polythiophenes, sulphur possesses lone pair of electrons that participate in aromatic sextet with delocalized π-orbitals. According to molecular orbital theory (MOT), when two atoms come nearby, the formation of some sort of bonds takes place, and they may combine right into a molecule, as a result of the interaction of the outer electronic orbitals having same or almost same energy. In the case of combined orbital system, the individual nuclei concurrently attracts the valence electrons. Hence, due the presence of atomic orbitals' interferences (constructive or destructive), their explanation can be done through new wave functions, named molecular orbitals. The constructive interference of orbitals results from the finite possibility of

locating the electron in between the nuclei. Such electron density involving the nuclei account of reducing of repulsion between the nuclei is connected with the reduced energy than either of atomic orbitals from which it's derived. Just because of promoting the atomic bonding, they are named as 'bonding molecular orbitals'. Oppositely to that, there is no chances of having the electrons, if the destructive interference takes place between two atomic orbitals. Without existent of any charge density (negatively charged) between the nuclei (positively charged), the account of more strong repulsion between the nucleii, is related to more considerable energy compared to the uncombined atomic orbitals. Thus, most of these orbitals are named as 'anti-bonding orbitals' which is having increased energy compared to that of bonding orbitals [Atkins et al. (2002)]. These bonding and anti-bonding orbitals are seems to be formed via division of single atomic energy level into two molecular energy levels within an energy level diagram. The formed anti-bonding molecular orbital is destabilized (due to more abundant energy than equivalent atomic orbitals, pressed upwards), whilst the bonding molecular orbital is stabilized (due to reducing energy than corresponding atomic orbitals, pressed down) [Atkins et al. (2002)]. The potency of the interaction between the atomic orbitals is indicated by the energy by which two orbitals are separated, and width of band is determined by robustness of inter atomic orbitals coupling. If the coupling is stronger then there will exist be the existence broader band, as more energy will takes place due to fragmentation. Thus the formation of valance band (VB) and conduction band (CB) takes into account due to presence of occupied orbitals and unoccupied orbitals respectively. Which further termed as Highest Occupied Molecular Orbital (HOMO), and another orbital is named the Lowest Unoccupied Molecular Orbital (LUMO) [Atkins et al. (2002)]. The energy difference between the HOMO in the VB and that of LUMO in the CB provides the energy gap, E_g.

The conventional polymers having sp^3-hybridized carbon atoms in backbone have a large band gap, making them electrically insulator, like reduced polyethylenes' optical band gap is of the order of 8 eV [Salaneck et al. (1999)]. Such kind of polymers having sp^3-hybridized carbon generally reveals large electrical band gap when compared with the polymers having sp^2 hybridized carbon. Polymers are having alternate single and double bonds (conjugated polymers) just like polyacetylene display comparatively low band gap. The band gap of conjugated polymers usually ranges between 1-4 eV [Gierschner et al. (2007), Jiang et al. (2011)], in precisely the same range as inorganic semiconductors lie. Because the conducting polymers have a bonding arrangement consisting of alternating single and double carbon bonds across the backbone of the polymer chain, this really is because of the valence band, and conduction band of conducting polymers are usually produced from such π-bonds, which is delocalized over the large segment of the polymer. This is actually the considerable difference between the conducting polymers and the polymers we frequently refer to as plastics. In the case of benzene polymer, the formation of a typical energy band diagram is revealed in Fig. 1.5 that is showing the overlapping of orbitals on the basis of increasing order of their energy as per molecular orbital theory. In general, the mechanism of carrier transport takes place through thermal hopping and tunneling of charge carriers to their neighboring states (localized) as well as mobility gaps in organic conjugated polymers (OCPs) [Dimitrakopoulos et al. (2002)]. The OCPs consist of the combination of alternate single and double bonds that result delocalized π-orbitals which are perpendicular to the molecular plane. The charge carriers are allowed to travel though these delocalized states to conduct the electricity. Hopping transport as well as band transport is basically two ways through which the carrier charge conduction takes place. Hopping transport mainly occurs in amorphous organic materials which are assisted by

phonons. These phonons get excited through the lattice vibrations and hence can tunnel among the neighbor molecules. Similarly, band transport mainly occurs in stable crystalline organic materials where the transportation of charge carrier transport takes place from HOMO to LUMO due to overlapping of the π-orbital in the OCPs energy band.

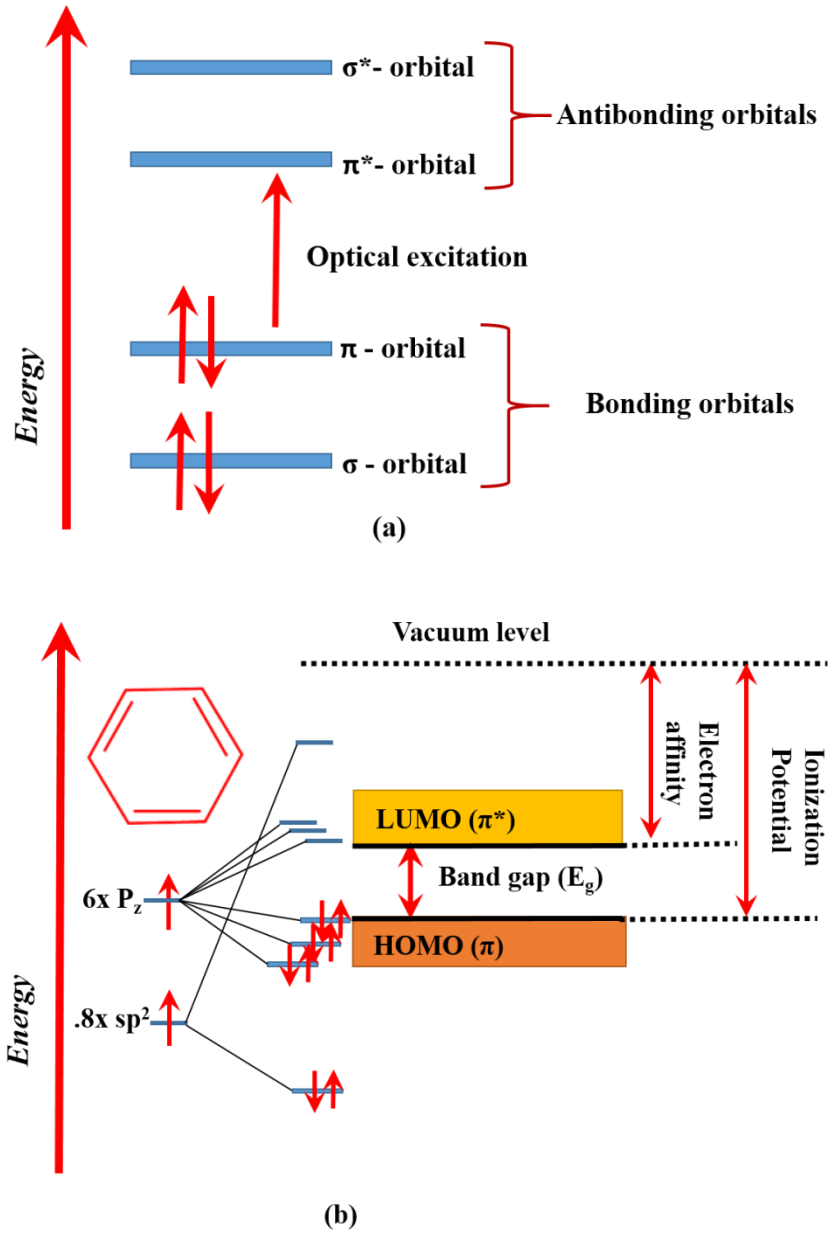

Fig. 1.5(a) The lowest electronic excitation (optical excitation) in the case of energy levels of a π-conjugated molecule, **(b)** Formation of bands with the separation of energy gap (by the collection of molecular orbitals)[Banerji et al. (2013), Christiansen et al. (1999)].

1.3 Doping in organic conducting polymers

Typically, conducting polymers exhibit poor conductivity (in the range of intrinsic insulators) in its reduced state. The free motion of π-electron around polymer chains isn't adequate to conduct electricity for almost any polymer. These π- electrons continue to be packed tightly on the polymer chain, and a number of them need to be eliminated or included from/to the conjugated backbone to create the electrically conducting. Thus; the drawback of poor conductivity can be overcome by creation of some defects into the polymer chains, the process is termed as 'doping'. In the doping process, the density of mobile charge carriers is raised, which leads to enhancement in the conductivity of conjugated polymers towards excellent conductor by modifying the dopant type, polymer regioregularity, blending of organic semiconductors and the doping level.

The electron elimination or addition accompanied by the association of oppositely charged ions (called dopant) to be able to keep the sum total charge neutrality results in doped polymers. This elimination (called p-type) and insertion (called n-type) result charge carriers on the polymer chain. The electrical conductivity results from the presence of charge carriers and their capability to maneuver across the π-bonded ''highway". Thus, doped conjugated polymers are excellent conductors for just two causes: (a) Doping propels carriers into the electronic structure. Conjugated polymers can be doped n-type or p-type to a comparatively large density of charge carriers [Chiang et al. (1978)]. (b) The charge-carrier mobility and carrier delocalization across the polymer chain is led by the attraction of an electron in one repeat unit to the nuclei in the neighboring units, which is prolonged into three dimensions through interchain electron transfer [Heeger (2001)].

The idea of doping in conjugated organic polymers is entirely different from the conventional semiconductor such as silicon. In the conventional semiconductors, a small

amount of a donor or acceptor is incorporated into the atomic lattice leading to the modification in the occupancy of the electronic states in the solid consequently of thermal ionization of the dopant. The band structure and the density of states are primarily unaffected by the incorporation of the dopant [Moore (1967)]. Nevertheless, doping of a conducting polymer includes the incorporation of a massive amount a donor or acceptor (more than 40 wt %). The involvement of such a massive amount dopant transformed the electronic, electrical, magnetic, optical, and structural properties of the polymer, which is considerably distinctive from the undoped material. The dopant perturbs the framework of the polymer thoroughly not merely due to its substantial physical size, and in fact it generally does not incorporate into the molecular structure, but in addition due to the considerable charge transfer occurs between the polymer chain and the dopant, resulting both to become ionic and ultimately causing alteration in the geometry of the chain. The doping level may also be reversibly managed to acquire conductivities ranging from the undoped insulating form to that of the completely doped, extremely conducting form of conducting polymers. With the help of an example shown in Fig 1.6 and Fig. 1.7, the addition of electron (n-doped) and removal of electron (p-doped) can be understand [Bredas et al. (1982), Johansson et al. (2003)]. In Fig. 1.6, the addition of negative charge species (commonly known as reduction) followed by recombination of free radicals result spinless solitons. Similarly, In case of Fig. 1.7, removal of electrons from thiophene backbone results polarons. These terminologies are explained latter in details.

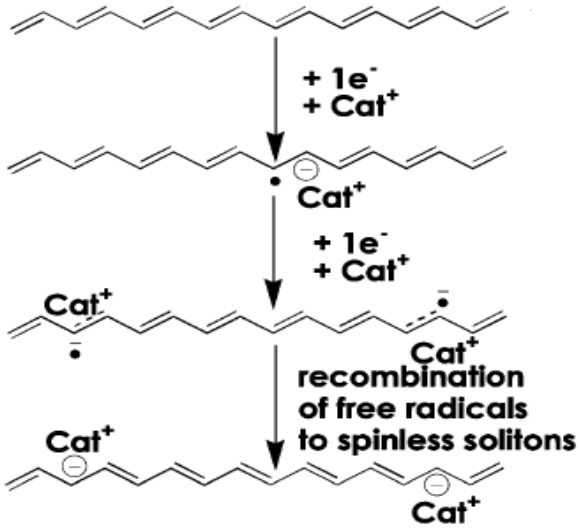

Fig.1.6 The process of doping (n-type) in case of poly (acetylene) [Bredas et al. (1982)]

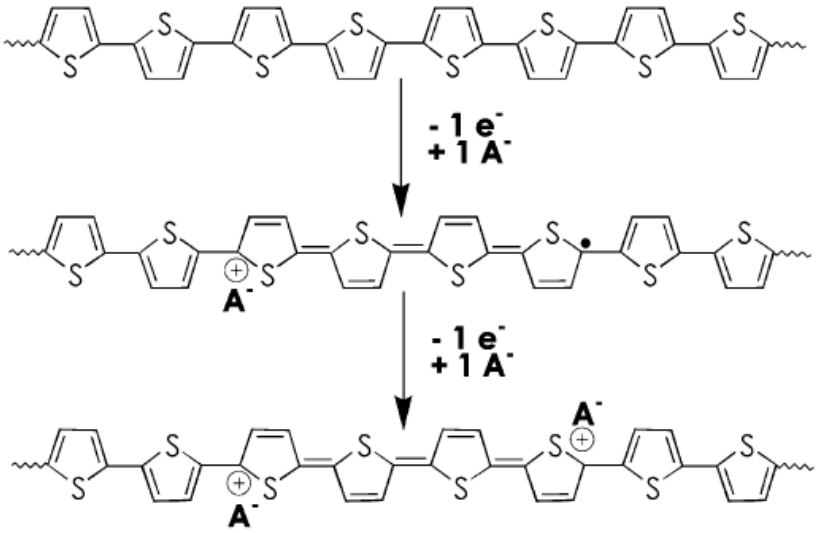

Fig. 1.7 The process of doping (p-type) in case of poly (thiophene) [Johansson et al. (2003)]

1.3.1 Types of doping: Polaron, bipolaron, and solitons

A particular form of charged defects formed on the polymer during doping is dependent upon the structure of the polymer chain. Primarily two significant categories of conjugated polymer backbones can be recognized: (1) one with degenerate ground state structures and

(2) other with non-degenerate ground state structures. After doping, if the energy of both structures (which formed as a result of local rearrangement of the bonding configuration) is same, it is termed as degenerate ground state. Usually, *trans*-polyacetylene exhibits such kind of degenerate state. Similarly, if the energy of both structures is not same, then it is termed as non-degenerate ground state. Both carbocyclic and heterocyclic polymers like polypyrrole, poaniline, polythiophene and its derivatives are eligible to exhibit such kind of energy states. Actually, in this concept, due to the formation of benzenoid and quinonoid bond sequence skeleton; where benzenoid bond sequence is having the lower energy as compared to the quinonoid bond sequence has; non-degeneracy occurs.

As compared to the inorganic semiconductors, the character of the charge carriers is entirely different in the case of conducting polymers. Unlike inorganic crystalline semiconductors, wherever charge transport takes place, generally by electrons in the conduction band and holes in the valance band, however, to describe the electronic phenomena in doped organic conducting polymers, new concepts including solitons, polarons, and bipolarons (charge carriers) have already been by solid-state physicists. [Moore (1967), Su (1979), Bredas (1985)]

The charge conduction in all the conjugated polymers arise with this phenomenon, including *cis*-polyacetylene, possesses non-degenerate ground states. When an electron is taken off from the π-system of polymer, a positive charge and a free radical (radical-cation) is produced. The radical cation is then combined by a regional bond rearrangement, and the formation of a quinonoid like bond sequence takes place, but limited distortions arise due to the higher energy of quinonoid lattice than that of benzenoid. In the case of polypyrrole, the lattice distortion is thought to outspread over four pyrrole rings as revealed in Fig.1.8.

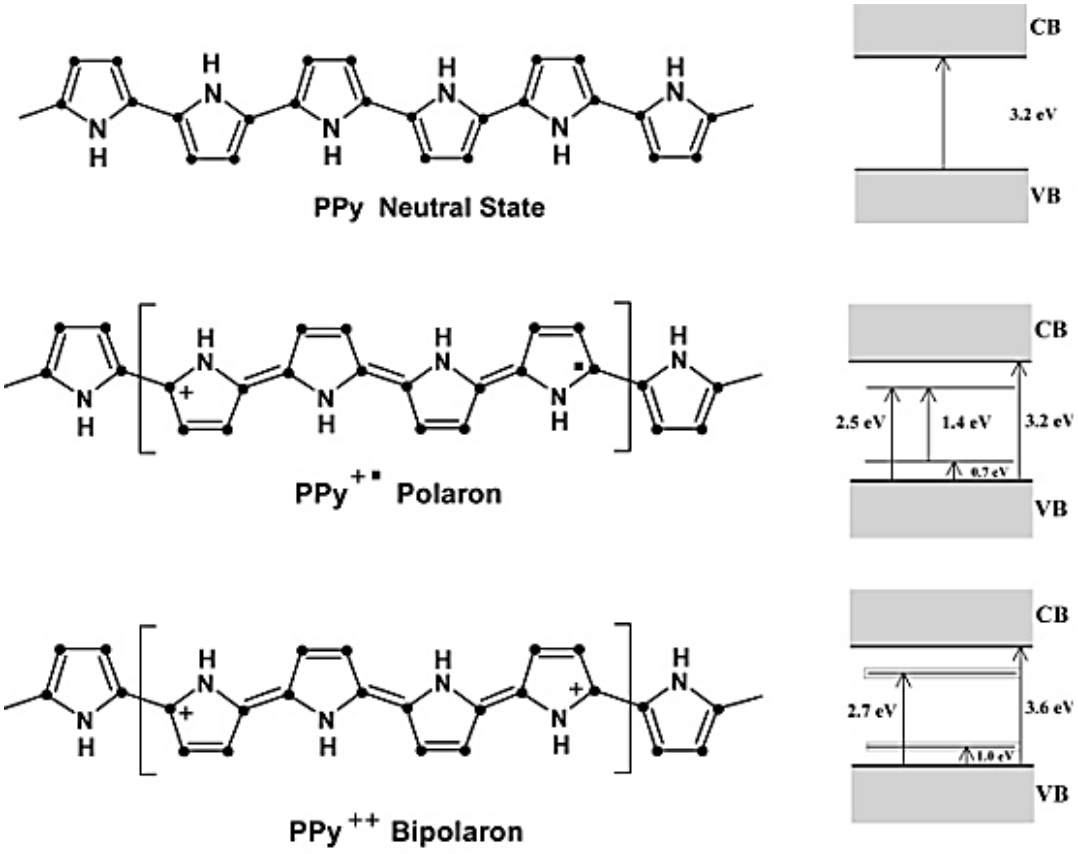

Fig.1.8 Formation of polarons and bipolaron in Polypyrrole [Kamloth (2008)].

This combination of the charged site coupled to a free radical with a regional lattice distortion is named a polaron. A polaron may be either radical anion (reduction) or radical cation (oxidation). The creation of localized electronic states in the VB and CB gap takes place by the formation of Polaron. As per the earlier reports, the polaronic states of polypyrrole are positioned (symmetrically) at 0.5 eV from the band edges [Bredas et al. (1985)]. The unpaired single electrons occupy the lower energy states. Additional oxidation may lead to the elimination of an electron either from the polaron or the rest of the chain. In the former case, polaron radical is removed, and new two positive charges result, which is coupled through lattice distortion. The formation of two polarons takes place in the latter case; on the other hand, the formation of bipolarons leads to the reduction in ionization

energy in contrast to two polarons. Therefore the former case is more thermodynamically favorable. There may be a possibility of production of a bipolaron by the combination of two polarons upon high doping. Empty bipolaron states are also positioned symmetrically within the band gap about 0.75 eV far from} the band edges in case of polypyrrole. Continuous doping of the polymer produces extra localized bipolaron states which overlap to create continuous bipolaron bands and provide metal-like conductivity.

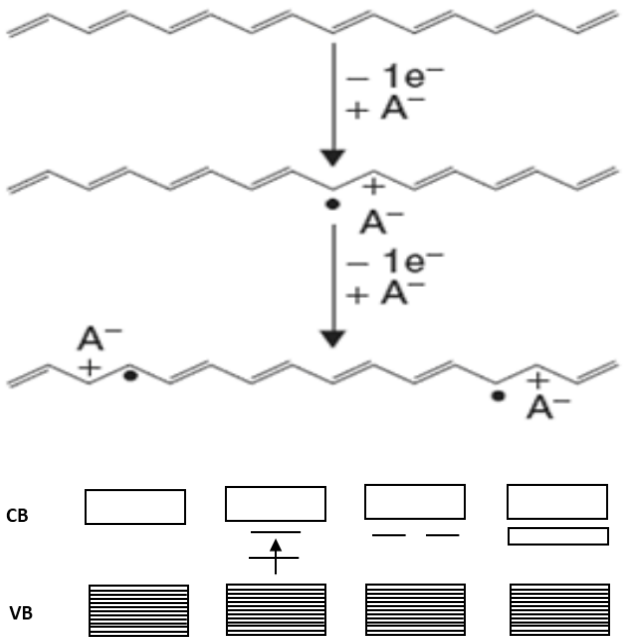

Fig.1.9 Formation of solitons in conducting polymers [Pron et al. (2000)]

The dissociation of bipolaron into the two spinless solitons is due to the presence of two equivalent forms of resonance (degeneracy) in the ground state of conjugated polymers like *trans*-polyacetylene (The *trans* form of polyacetylene is unique among conducting polymers because of the presence of two geometric structures of the same total energy). As a result of this degeneracy, the two charges forming the bipolaron in *trans*-polyacetylene can readily separate (Fig. 1.6). Such a phenomenon is analogous to the charge associated

with the boundary of domains walls in case of inorganic materials. Such a charge associated with a boundary or domain wall is called a soliton. The presence of a soliton leads to the appearance of a localized electronic level at mid-gap, which is half-occupied in the case of a neutral soliton and empty (doubly occupied) in the case of a positively (negatively) charged soliton (Fig.1.9). Compared to a polaron, the soliton has an unusual spin-charge relationship: since a neutral soliton is radical, it has a spin 1/2 whereas a charged soliton is spinless.

1.3.2 Methods of doping

The injection of charge into macromolecular polymeric chains is led by doping of conjugated polymers, are generally, of five types as represented in Fig.1.10. [Van Mullekom et al. (2001), Tomlinson et al. (2014), Kaneto et al. (1985)].

(I) Chemical doping -

The chemical doping mainly comprises of either chemical oxidation or reduction of the polymer backbone. The oxidation process leads to the removal of electrons and generates a positively charged polymer while reduction produces a negatively charged backbone. These doping processes are referred as ‘p-doping and ‘n-doping' respectively [Chiang et al. (1977), Chiang et al. (1978), Shirakawa et al. (1977)], and can be understood by following examples:

(a) p-type:-

$(\pi\text{-polymer})_n + 3/2\ ny\ (I_2) \rightarrow \{(\pi\text{-polymer})^{+y}\ (I_3^-)_y\}_n$

The other common dopants are ClO_4^-, SO_4^{2-}, Halides (X^-=Cl^-, Br^- F^-), BF_4^- etc.

(b) n- type:-

$(\pi\text{-polymer})_n + \{Na^+(Naphthalid)^-\}_y \rightarrow \{(Na^+)_y (p)^{-y}\}_n + (Naphth)^0$

The other common dopants are alkali metal ions, Li^+, Ca^{2+} etc.

When the doping level is sufficiently high, the electronic structure evolves to that of a metal.

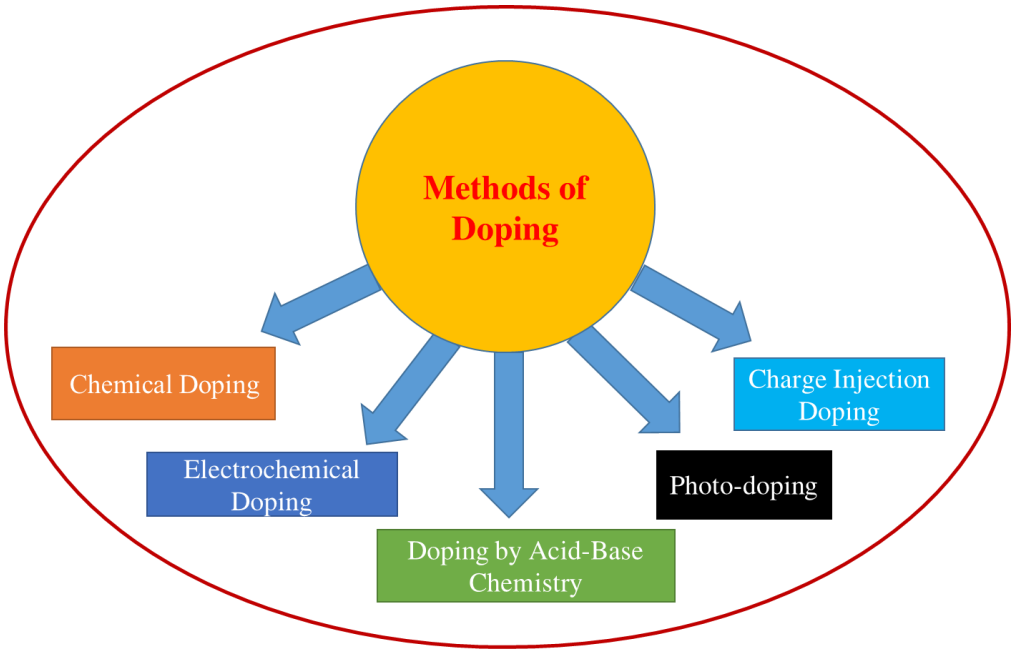

Fig. 1.10 Various methods of doping process.

(II) Electrochemical doping –

It is no doubt that, the chemical doping is definitely an effective, easy and cheap method for doping the polymers. However, in this technique, the extent of doping is hard to control while sometimes efforts to acquire intermediate doping levels usually lead to formation of inhomogeneous doping. Therefore, concept of electrochemical doping came in picture in order to remove this issue. [Nigrey et al. (1979)]. The electrochemical doping process is a similar way of doping like chemical doping, except the driving force for the oxidation and reduction is supplied external voltage source (i.e., by the electrochemical potential of the

working electrode). Electrochemical p-type and n-type doping can be achieved beneath anodic and cathodic situations respectively. In p-type and n-type doping techniques, the positive and negative charges on polymers stay delocalized and are balanced by the incorporation of counter ions (anions or cations) which are illustrated as dopants. Herein, the doping level is controlled by the applied voltage. Electrochemical doping is explained by the following examples:

(a) p-type

$$(\pi\text{-polymer})_n + [Li^+ (BF_4^-)]_{sol'n} \rightarrow [(\pi\text{-polymer})^{+y} (BF_4^-)_y]_n + Li\ (electrode)$$

(b) n-type

$$(\pi\text{-polymer})_n + Li\ (electrode) \rightarrow [(Li^+)_y (\pi\text{-polymer})^{-y}]_n + [Li^+ (BF_4^-)]_{sol'n}$$

(III) Doping by acid-base chemistry -

This type of doping is referred to as non-redox doping in which a number of the electron associated with the polymer backbone does not change during the doping process. For example, protonation by acid-base chemistry leads to an internal redox reaction and the conversion from semiconductor to conductor. The protonation of polyaniline is typical examples of such kind of doping process (Fig. 1.11). The chemical structure of the emeraldine base form of polyaniline is that of an alternating copolymer. Upon protonation of the emeraldine base to the emeraldine salt, the proton-induced spin unpairing mechanism leads to a structural change with one unpaired spin per repeat unit, but without a change in the number of the electron [Wudl et al. (1987); MacDiarmid et al. (1990)]. The result of a half-filled band potentially leads a metallic state in which there is a positive charge in each repeat unit (from protonation) and an associated counterion (e.g., Cl-, HSO4-, DBSA-, etc.).

(IV) Photo-doping -

This type of doping is different from the above-described doping phenomena, where no counter dopant ion is involved. The semiconducting polymer is locally oxidized and reduced by photo-absorption. Photo-doping is described by the following examples:

$$(\pi\text{-polymer})_n + h\nu \rightarrow [\{\pi\text{-polymer}\}^{+x} + \{\pi\text{-polymer}\}^{-x}]_n$$

where, x is the number of electron-hole pairs. If the potential is applied during photoabsorption, then electrons and holes separate and photoconductivity is observed.

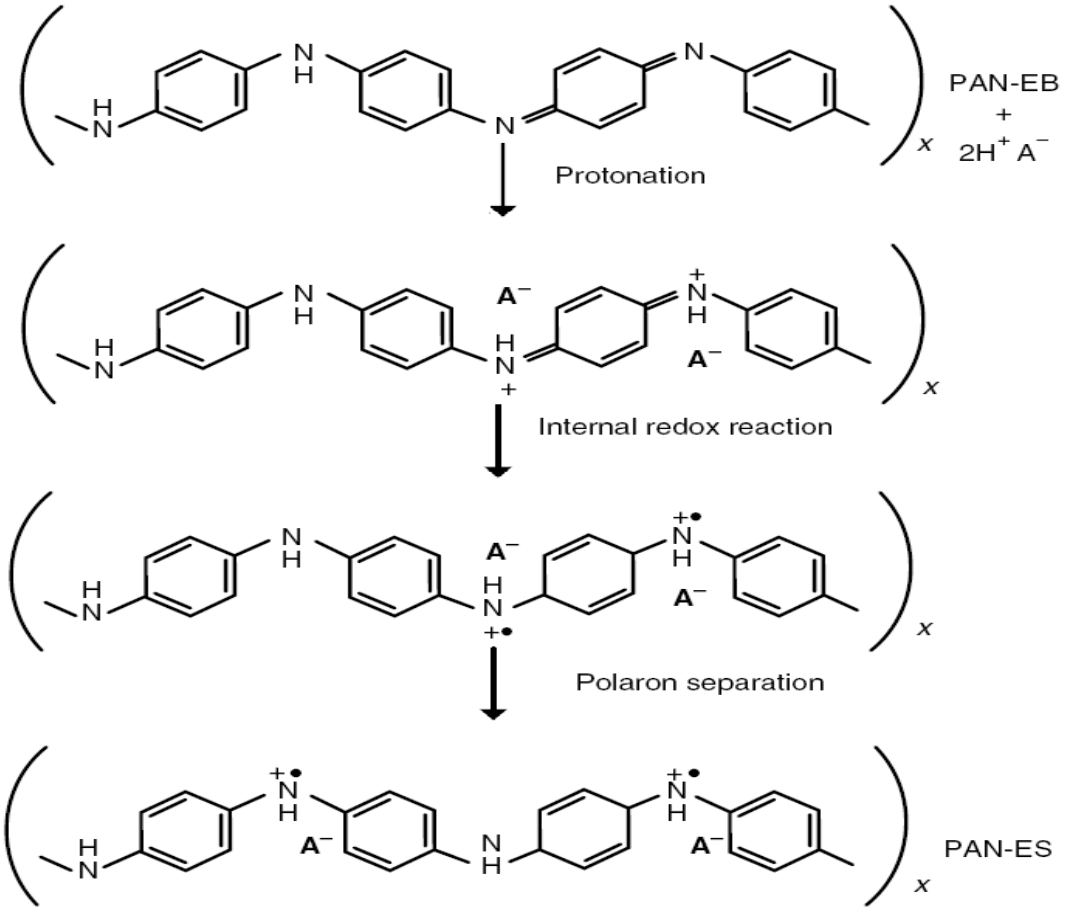

Fig. 1.11 Doping Mechanism in polyaniline by acid-base chemistry [Skotheim et al. (2007)]

(V) Charge injection doping -

In this type of doping there is no counter dopant ion is involved like photo doping. This type of doping is usually observed at the metal-semiconductor (M-S) interface, where electrons and holes can be injected from metallic contacts into the π^* and π bands, respectively. In the case of charge injection doping the polymer is oxidized or reduced (electrons are added to the π^* band or removed from the π band) at M-S interface. The methods of charge injection doping leads to unique and important phenomena in the polymer semiconductor as the active element in thin-film diodes [Tomozawa et al. (1987) and (1989)], polymer light emitting diode (PLED) [Burroughes et al. (1990)] and polymer field effect transistor (PFET) [(Burroughes et al. (1988), Garnier et al. (1994), Drury et al. (1998)].

1.4 Polyalkylthiophenes (PATs): A potent polymer for engineering purpose

PATs are class of heterocyclic organic conducting polymers which contains thiophene ring and alkyl chain in its monomer. It was first synthesized in the year of 1980 (2-5 coupled polythiophene) [Lin et al. (1980)]. Several derivatives of PATs have already found their applications in the electronic industry, and many are being explored for their usability. The conjugated PATs shows better conductivity and ambient stability with respect to other conducting polymers such as polyaniline and polypyrrole [Li et al. (1993), Lungenschmied et al. (2007)]. The PATs can be synthesized via both electrochemical depositions as well as chemical routes which is insoluble in common organic solvent because the backbone rigidity, higher crystallinity, and enhanced intramolecular interactions make PATs generally insoluble in commonly used organic solvents like xylene, toluene, trichlorobenzene, chloroform, etc. This insolubility limits solution processability. It also

prohibits uniform doping in PATs. Because of these bottlenecks, it is generally difficult to make semiconducting/conducting polymers. In order to make the semiconducting/conducting PATs, they should be exposed to the dopant vapor or liquid during the electrochemical deposition itself. In common practice, it was challenging to have precise control of doping concentration and uniform doping. These are some significant limitations of PATs, which restricted their applications in organic electronics.

The insolubility of these PATs in common organic solvent suppress not only the uniform doping but also its processability on the desired substrate using particular processing methods such as printing, spin coating, casting, etc., It is also apparent that the mandatory condition for the fabrication of high efficient devices (PTs based), is the uniaxial orientation of crystallites and this particular orientation can only be acquired through solution processing by implementing several growth methods [Nagamatsu et al. (2003), Pandey et al. (2013), Jimison et al. (2008)] because the maximum mobility is along the polymer backbone. The challenging issue related to the PATs solubility was first resolved in the year 1987 by Hotta et al. They grafted an alkyl side chain over specific position (3^{rd}) of the thiophene rings; and entitled as poly (3- alkylthienylenes). (P3ATs) [Hotta, (1987)]. Furthermore, it's also reported that the enhancement in the solubility can be seen by the inclusion of as-long alkyl side chains. [Gurau et al. (2007), Hancock et al. (2008)]

1.4.1 The alkyl side chains

The basic intension of having Alkyl side chain in conjugated polymers is to provide solubility. The molecular formula of Alkyl chains is $-C_nH_{2n+1}$ (n denotes the number of carbon atoms). Alkyl chain can be classified into linear, cyclic, as well as branched alkyl chains (Fig. 1.12). In the case of linear alkyl chains, the most common chain are hexyl,

octyl, and dodecyl. Statistically, linear alkyl chains with even numbers of carbon atoms are more popular than those with odd-numbered carbon atoms, presumably due to their commercial availability. The length as well as the specific position of alkyl chain matters in the sense to promote the interdigitation (interchain). The interesting fact associated with these side chains is that they possess good solubilizing capability without disrupting the π–π interactions of the main polymer chain.

These features are especially crucial when one design conjugated polymers for electronic charge transport properties. The sort of alkyl chain influences a polymer's conformations and molecular packing, the position of these chains on the conjugated backbones also regulates these parameters. The regioregular poly (3-aklylthiophene) (rr-P3AT) and regioirregular (regiorandom) analogue are well-known cases of this effect. rr-P3ATs have a homogeneous polymer backbone with nominal steric hindrance from the adjoining alkyl chains. But, the regiorandom P3ATs have heterogeneous and arbitrarily twisted backbones due to the steric hindrance arising from the mutual interactions of neighboring alkyl side chains. In the case of rr-P3AT based thin film based transistors (TFTs), the carrier mobility is enhanced by 2 to 3 order with respect to its regiorandom counterpart. Modification in the position of alkyl chain leads to the alteration in the properties of polymers. Nevertheless, in the case of conjugated backbones, the placement of alkyl side chain is restricted to specific available positions.

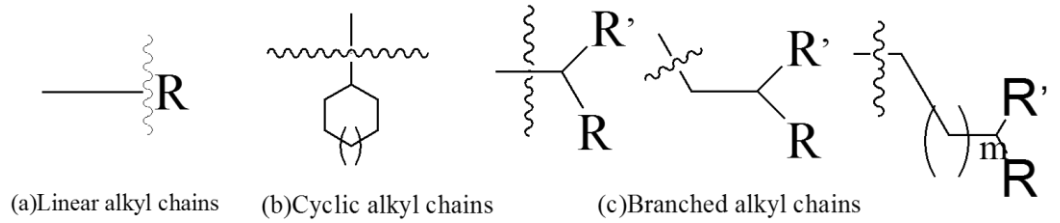

Fig. 1.12 some example of side chains (a) Linear alkyl chains (b) Cyclic alkyl chains (c) Branched alkyl chains.

1.4.2 Regioregularity

It is a spatial coupling of monomers in a polymer backbone so that alkyl chains are arranged in particular manner. It can be seen in the structural formula 3-hexylthiophene shown in Fig. 1.13(a). PAT that contain significant number of head-to-head (2, 2' coupling) (Fig. 1.13(b')) or tail to tail couplings (5, 5' coupling)) (Fig. 1.13(b')) are referred to as regio-irregular (regiorandom), while polymers that contain only head-to-tail couplings (2,5' coupling))(Fig. 1.13(c)) are referred to as regioregular. The basic differences between regio-irregular and regioregular structural formula have been shown in Fig. 1.7(b, b', and c)).

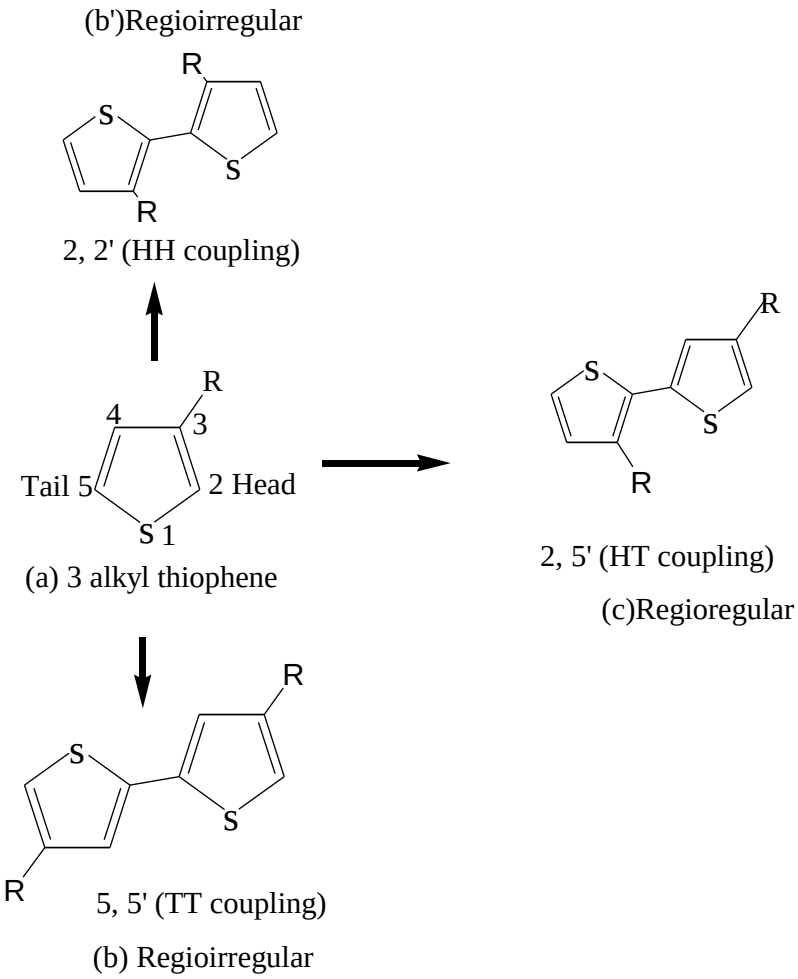

Fig. 1.13. Structural formula of (3- hexylthiophene) (a), regioirregularpoly(3 hexyl thiophene) (b) (b'), and regioregular poly(3 hexylthiophene) (c), respectively.

Regioirregular polymers cannot adopt planar conformations, and irregular placement of the solubilizing alkyl substituents limits the efficient solid-state packing and materials physical properties. In contrast to regioirregular polymers, regioregular, head-to-tail coupled poly (3- alkylthiophenes) (HT-PATs) can undergo self-assembly, in solution as well as in the solid phase. Such an assembly generally results in highly ordered two- and three-dimensional polymer architectures, thus, making these materials to have superior electronic and photonic properties when compared to their regioirregular analogues.

1.4.3 Orientations in PAT chains: Edge-on, Face-on, and End-on

The orientations of PATs polymer chains crystallites over the solid substrate can be distinguished according to polymer backbone orientations. There are three possible orientations of polymer chains over the solid substrate.

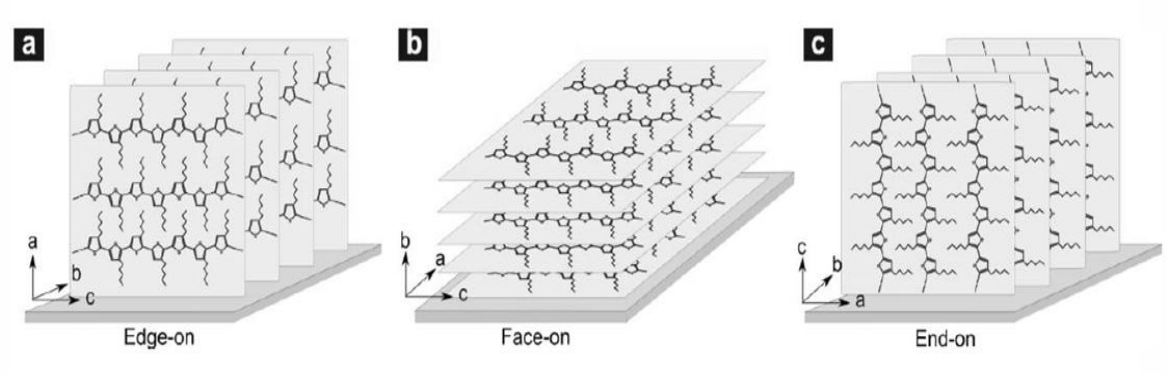

Fig. 1.14. Edge on (a) face on (b) and, Flat-on (c) orientation of regioregular PATs (Salammal(2012), Pandey (2017)).

The π-π stacking direction of the PATs crystallites, confirms its orientation, like if it is parallel to the substrate then edge- on orientation occurs (Fig. 1.14(a)) and when its perpendicular to the substrate face-on oriented orientation of crystallite occurs (Fig. 1.14(b)). These two types of orientation are very common in regioregular polymer chains. In a very rare case, the End-on orientation of P3AT nanocrystallites occurs. The PATs

polymer chains in crystallites lie along the perpendicular to the substrate called flat-on oriented crystallites (Fig. 1.14(c)). [Brinkmann et al. (2007)]

1.4.4 Charge transport in oriented PATs:

The derivatives of thiophene-based organic conducting polymers (OCPs) are well known for their better stability, processability, enhanced mobility etc., and hence they are performing the crucial role in the fabrication of electronic devices. The charge transport in regioregular PATs crystallites is completely anisotropic. It has been observed that the electrical conductivity favors in high extent along the polymer backbone (conjugation direction; intrachain hopping) or along the π-π stacking direction (face-on orientation; interchain hopping). This can be understood by the typical example shown in Fig.1.15. The phenomenon of conduction through conjugation length as well as the through hopping can be much effective in the charge transport when the OFETs are fabricated specially by edge-on oriented crystallites (as schematically shown in the Fig. 1.15). In this case hopping is quite different as the hopping and tunneling process taking place into two regions having disordering, here it denotes the charge transport between the lamella having the specific ordering. So, in the view of OFETs, these specific orientation in crystallites (especially edge-on) can be liable for the better conduction of electricity by means of conjugation (through polymer backbone) and interchain stacking (through hopping in interchain transport). In such case the edge-on oriented crystallites can help to produce high-efficient OFETs as compared to other counterparts because of restricted charge transport along the alkyl side chains due to its insulating nature.

Theoretically, it is well known that charge conduction along the oriented PATs backbones is limited up to certain contour length. Here high molecular weight as well as orientation of

regioregular PATs comes into picture to play vey decisive role in the charge transport. Both the factors favor the enhancement in the carrier mobility by providing the interconnection between the crystalline domains (prevents the trapping of charge carriers in disordered regions/grain boundaries) as well as by increasing the contour length. But at the same time, the high molecular weight of polymer increases the chances of backbones-folding. Similarly, polymer thin films are of semi-crystalline nature. Where the nanocrystallites are embedded into the amorphous matrix.

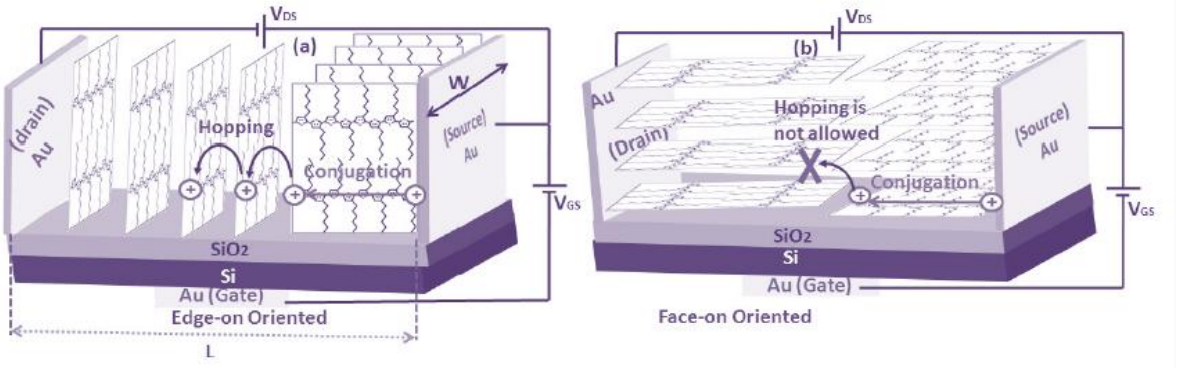

Fig. 1.15. Charge transport in OFET fabricated using (a) edge- on oriented and (b) face -on oriented polymer chains. (Salammal(2012), Pandey (2014)).

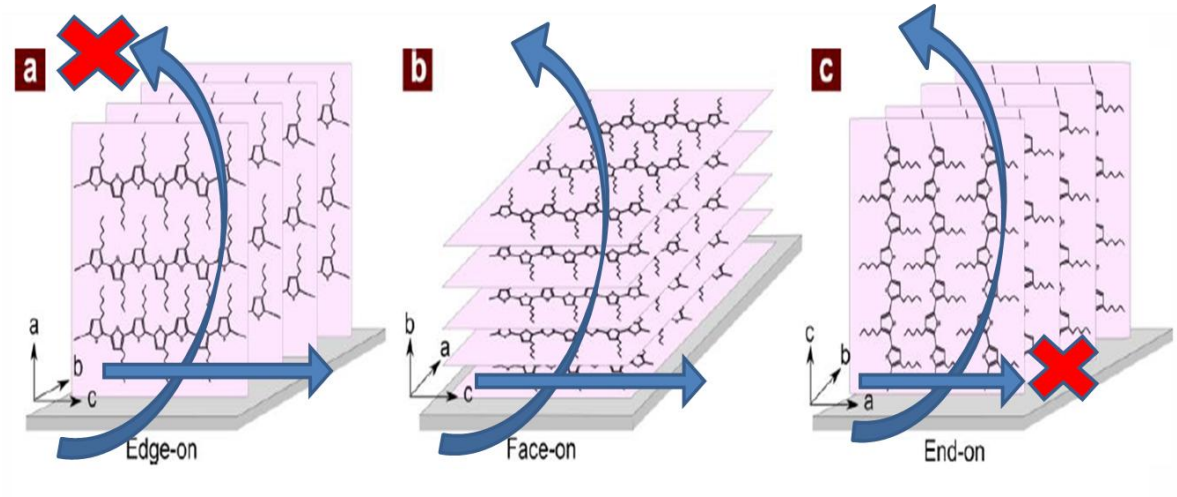

Fig. 1.16. Charge transport in PAT sandwiched diode fabricated using (a) edge- on oriented, (b) face -on oriented and (c) end-on oriented polymer chains.

So, in the case polymeric thin films, the main factors to hamper the charge transport are (a) poor in-plane stacking, (b) poor crystallinity, (b) grain boundaries, etc. [Sirringhaus et al. (2000), Nagamatsu et al. (2003), Pandey et al. (2013), Jimison et al. (2008)]

Similarly in the case of vertical diodes, the face-on orientation with respect to substrate exhibits better charge transport than that of end-on or edge-on (the scenario is as depicted in the Fig. 1.16**)**. This is due to direct overlapping of conducting π-electrons with metal electrode's surface [Singh et al (2017)].

1.4.5 Various strategies for orientations of PATs

There are various types of strategies have been adopted till the date (as shown in Fig.1.17). Basically, all these efforts involve orientation of PAT chains to each other. For example solvent assisted orientation like ageing, poor solvent induced assembly, pressure dependent assembly, thermal annealing, high temperature rubbing, assembly by solvent evaporation, FTM etc., solvent or liquid surface plays decisive role for the slow aggregation of polymer chain from its disentangled state (in true solution state).

Among these strategies, we employed two techniques *viz.* ageing and marginal solvent driven assembly, due to its effortless (easy) experimentation, and require no sophisticated lab (cost-effective). Ageing process involves slow aggregation of polymers from its disentangled state into the lowest energy aggregated state with span of time. Similarly, in other process also involves slow aggregation of polymers from its disentangled states in good solvent into the lowest energy aggregated state under the influence of poor solvent.

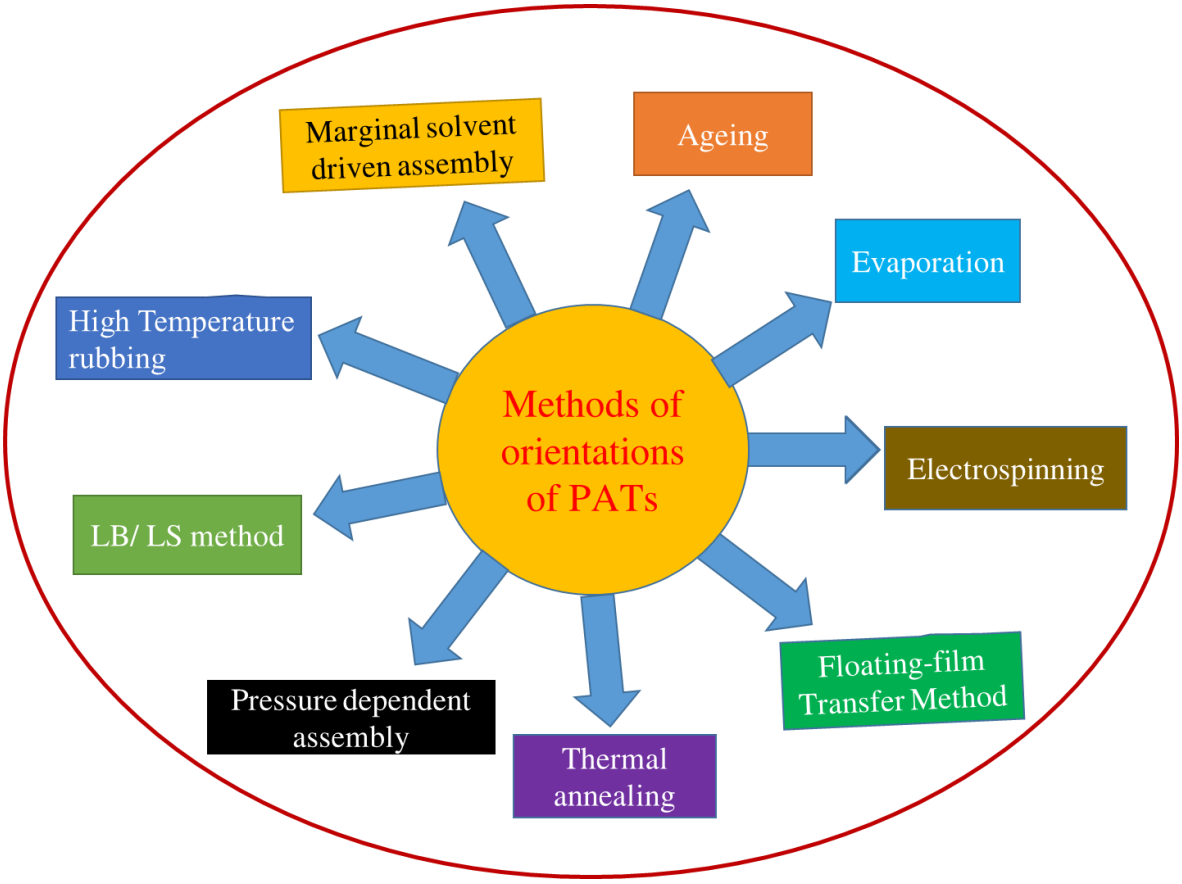

Fig.1.17. Various methods of orientation of PATs.

1.4.6 General aspects of rr- P3HT, rr-PQT-12 and rr-pBTTT-C14

rr-P3HT, rr-PQT-12 and rr-pBTTT-C14 are of semiconducting PATs derivatives which are structurally different though coupling of thiophene moieties as shown in Fig1.18. One monomeric unit of rr-P3HT consist of one thiophene ring with hexyl side chain at its 3-position. rr-PQT-12 consists of a monomeric skeletal having four thiophene rings with two dodecyl side chains attached at 3, 3''' positions. Similarly, the monomer of rr-pBTTT-C14 has also four thiophene skeletal type but two middle thiophene rings is fused together and tetradecyl side chains are attached at same location about this fusion. These polymers have attracted more interest due to their higher stability in air and processability in common solvents like, chloroform, toluene, xylene, anisole etc. comparison to other polymers like

polyaniline, polycarbazole, polyindole etc. At the same time, the increment in the carrier delocalization may be expected due to greater degree of structural ordering which leads to enhancement in the mobility. Therefore, a suitable comprehension of the aspects, governing the electronic and atomic framework will undoubtedly be much beneficial in controlling the synthesis of new polymers. Furthermore, development in the design of the material on the atomic range may cause to improved mobility inside a crystalline region. On evaluating Fig. 1.18a and Fig. 1.18b, the major dissimilarity between rr-P3HT and rr-PQT-12 is identified by the arrangement as well as density of the side chains. The density of alkyl side chain (in rr-PQT-12) is lowered as compared to rr-P3HT, and the length of the c-axis is twice as long in rr-PQT-12. Similarly, the chemical structure of rr-pBTTT is shown in Fig.1.18 (c). Here, each monomer comprises two thiophene rings and one fused ring. There are two alkyl side chains C_n attached in a head-to head arrangement on neighboring thiophene rings. By comparing the structures with rr-P3HT and rr-PQT-12, it can be observed that by the removal of two carbon atom per monomer and additionally fusing them, one can obtain rr-PBTTT-C14 easily. Apart from this, fourteen carbon atoms associated with this structure, refers it to be termed as rr-pBTTT-C14. Recently, the polymer series rr-pBTTT-C_n was reported to exhibit field-effect mobility in the range of 0.2–0.6 cm^2 /Vs [Northrup (2007)]. The current result pulls the attraction to work with rr-rr-pBTTT-C_n because of having improved mobility as compares to rr-P3HT and rr-PQT-12, which is mainly because of the better rigidity of polymer backbone, contributes to the better planarity and hence better molecular packing which avoids the steric hindrance which usually occurs in the case of rr-P3HT.

The assessment of enhanced mobility in polycrystalline rr-pBTTT-C14 might be a consequence of better mesoscopic ordering and certainly not a consequence of the

variations in the local atomic structures. The calculations suggest that interdigitation of the alkyl chains in rr-pBTTT-C14 is actively promising. Thus, polymers that have the ability to interdigitate excellently may possibly be anticipated to present a better structural stability. It has been observed that, rr-PQT-12 with long dodecyl chain substitution on the polymer backbone allows both solution processability and molecular self-organization in solution. In addition, the backbone also allows extended π-conjugation and oxidative stability, making it a suitable semiconductor material for organic devices.

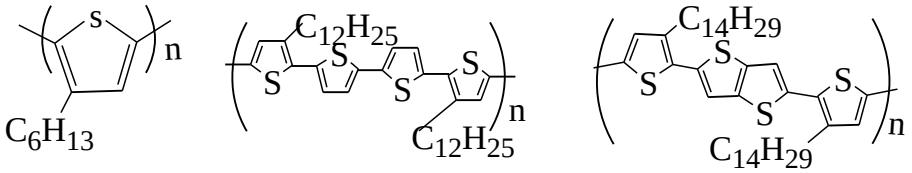

(a)Poly(3- hexyl thiophene)

(b)Poly(3,3‴- dialkyl quarter thiophene)

(c)Poly(2,5-bis(3-alkylthiophen -2-yl)thieno[3,2-b]thiophene)

Fig. 1.18. Structural formula of (a) poly(3- hexylthiophene) (b) Poly (3,3‴-didodecylquarterthiophene) (c)Poly(2,5-bis(3-alkylthiophen-2-yl)thieno[3,2-b]thiophene).

1.5 General terminologies on conducting polymers/metal interface

The research field of organic electronics experiences tremendous developments since the discovery of conducting polymers and the developments of applications where organic materials replace the traditionally used inorganic semiconductors. Devices such as field-effect transistors (OFETs), light-emitting diodes (OLEDs) and solar cells (as shown in Fig. 1.19) based on organic conjugated materials as active materials represent the key applications of the domain. FET is three terminal devices (source, drain, and gate), by controlling the voltage on one plate (the gate), a charge can be induced on the other. These charges are injected from the source electrode and collected across the conducting channel at the drain by applying a voltage between the two. The injection of charge from source

and collection of charge from the drain electrode is strongly depending on the types of the barrier formed between them.

Similarly, in OLEDs, charge carriers (holes and electrons) are injected from the electrodes into the organic semiconductor and emit light when they meet, as shown in Fig.1.19. Solar cells have an opposite working principle compared to OLEDs: light is absorbed and dissociated in charge carriers that migrate to the electrodes to give rise to electric current as shown in Fig. 1.19. The gain of better device performances (better conversion efficiency for OLEDs and solar cells or high ON/OFF ratios for OFETs) requires a better understanding of interfaces between organic materials and electrodes. The electronic phenomenon at the interface is critically important to the performance and function of such devices. Therefore, it is necessary to understand not only the properties of conducting polymers itself but also interfacial electronic phenomena.

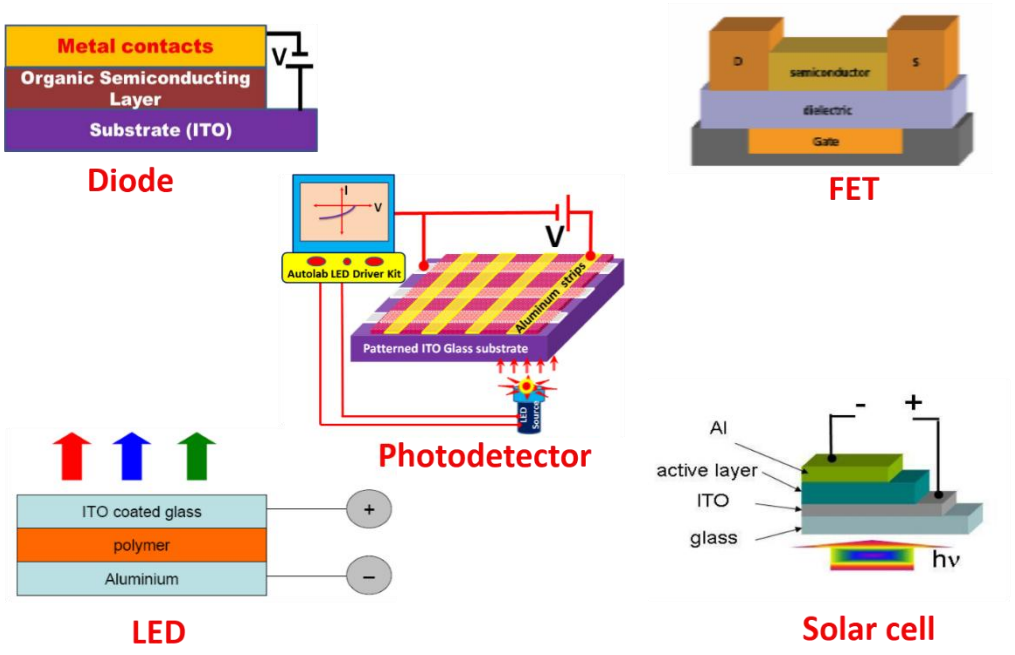

Fig.1.19. Some examples of electronic devices based upon polymer /metal interface

1.5.1 Metal–Semiconductor interface

The metal-semiconductor (M-S) interfaces are the essential component of almost all electronic and optoelectronic devices. One of the most interesting phenomena is the formation of the Schottky barrier, which is the measure of mismatch of energy levels of majority carriers across the metal-semiconductor interface. The first practical semiconductor device was the metal-semiconductor contact in the form of a point contact rectifier, that is, a metal pressed against a semiconductor surface. The rectifying effect in metal-semiconductor contact diodes was discovered in 1874 by F. Braun and was explained by Schottky and Mott in 1938. Schottky proposed that the potential barrier is prime factor to develop the rectifying behavior due to presence of stable space charges in the semiconductors. Metal-semiconductor interface may also be non-rectifying; that's because of contact includes a minimal resistance irrespective of applied voltage polarity. Such contact is known as an ohmic contact. The question arises here how a junction can be ohmic or rectifying. The way to find a junction ohmic or rectifying depends on the work function of metal and semiconductor. The work function of a substance is the energy required to bring an electron from the Fermi level to the vacuum level. Therefore, we will demonstrate this using the band diagram and show how the potential barrier is formed at the junction. This potential barrier will be responsible for a contact to be ohmic or rectifying and will be discussed in next coming sections. Here is a Table 1.2, demonstrating the electrical behavior of the device.

Table 1.2 Contact Characteristics

Semiconductor	**Ohmic**	**Rectifying**
N type	$\Phi_M < \Phi_S$	$\Phi_M > \Phi_S$
P type	$\Phi_M > \Phi_S$	$\Phi_M < \Phi_S$

1.5.2 Theory of Schottky /Ohmic contacts-

Schottky diodes vary from conventional (PN-junction based) devices because of rectification takes place as a result of big difference in work-function involving the metal contact and that of the semiconductor, instead of having a non-uniform doping profile. In the semiconductor, the recombination of minority charge carriers does not control the Conduction. Here the conduction is controlled by thermionic emission of majority carriers over the barrier developed by the difference in work-functions. Hence the Schottky diode is can be termed as a majority carrier device whose switching rate is not confined by minority carrier effects.

Schottky barrier

Case -1 for n-type semiconductor and uniformly doped, when $\Phi_M > \Phi_S$

During the formation of contact between metal and semiconductor, the flow of electrons takes place from conduction band of semiconductor to metal due to presence of higher energy electrons in semiconductor. This phenomenon ends until Fermi levels of the both are perfectly aligned. This flow of electrons from semiconductor to metal, leaves behind the ionized donors (positively charged). Finally due to electrons accepting property the metal acts as ionized acceptor (negatively charged), at thermal equilibrium. Due to the presence of positive and negative charges, the formation of a dipole layer takes place that is

quite to that in a p^+-n junction where the Fermi level is constant throughout the entire metal-semiconductor system, and formed energy band diagram is quite similar to that for an n-type semiconductor in a p^+-n junction. These positive charges extended up to a thickness W in the semiconductor. However, the negative charge on the metal side is contained within a distance of about an atomic layer and is essentially a surface charge. Furthermore; an electric filed is developed (from semiconductor to metal) due to this dipole layer of charges. There are three basic rules (given below) which govern the shape of the energy band diagram of the metal-semiconductor junction.

(*i*)-In equilibrium, the Fermi levels for the semiconductor and metal must be constant throughout the system;

(*ii*)-The electron affinity must be constant (χ, which is defined as the energy difference between the bottom of the conduction band to vacuum level);

(*iii*)-The free-space energy level must be continuous.

To be able to meet all three rules (above stated) concurrently, the valence and conduction bands of the semiconductor are forcibly bent at the junction; the upward bending of the conduction band of the N-type semiconductor suggests the formation of depletion region, also resulting the formation of potential difference across the region which is merely the difference of work-functions of the both, as depicted in the Fig. 1.20,

$$qV_{bi} = \Phi_M - \Phi_S$$

This difference of work-function are further termed as the junction the built-in potential. Further the barrier height Φ_b (metal toward semiconductor) can be calculated easily by-

$$q\Phi_b = q\left(\Phi_M - \chi\right)$$

$$= qV_{bi} + \left(E_C - E_F\right)$$

Since $q\Phi_S = q\chi + \left(E_C - E_F\right)$

In the thermal equilibrium at temperature T, a small fraction of conduction band electrons will have sufficient energy to surmount the barrier. These electrons flow into metal, and current flow from the metal to semiconductor. This current is exactly balanced by an equal and opposite current caused by the electrons flow from metal into the semiconductor. If the biasing of the semiconductor is negative (by voltage V_F) as compared to that of metal, the decrement in the built-in potential (from qV_{bi} to q (V_{bi} -V_F)) takes place for the electron in the semiconductor. This leads to flow of more electrons from semiconductor to the metal which is liable to increment in current beyond its thermal equilibrium value. Nevertheless, since $q\Phi_b$ remain almost unchanged, there is no change in the value of current (exists net flow of current) from semiconductor to metal due to no voltage drop across metal. Conversely, the reverse bias (V_R) reduces the electrons flow from the semiconductor to the metal, and hence reduces the current (from metal to a semiconductor) below its equilibrium value whereas current from semiconductor to metal remain almost unchanged as shown in Fig. 1.21.

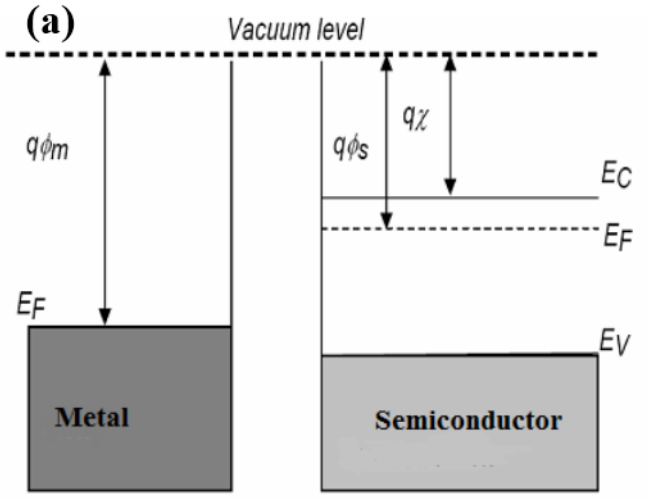

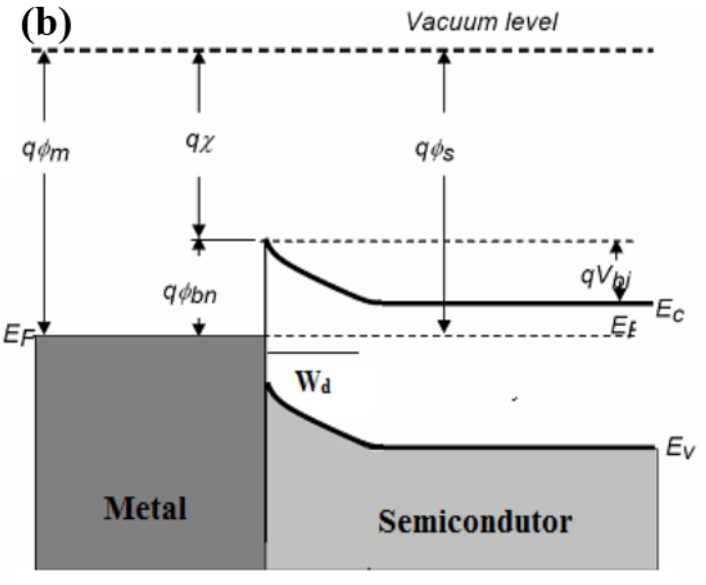

Fig.1.20. Energy level diagram of metal and semiconductor (a) before the contact (b) after the contact [Singh (2010)]

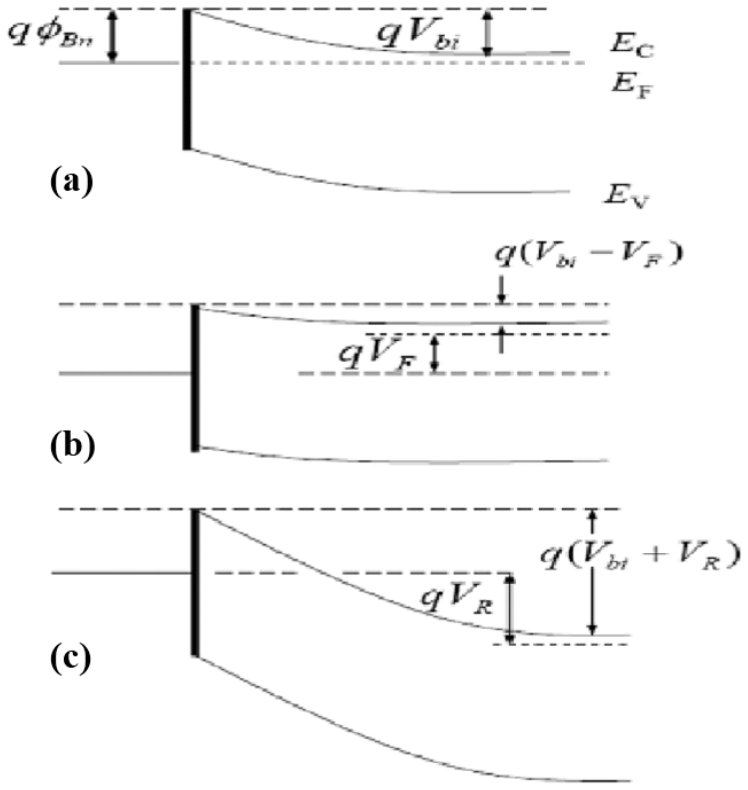

Fig.1.21. Energy level diagram of metal/semiconductor (n-type) interface under (a) thermal equilibrium (b) forward biasing and (c) reverse biasing [Sze (1981)].

Case -2 for p-type semiconductor and uniformly doped, when $\Phi_S > \Phi_M$

In this case, during the formation of contact between metal and semiconductor, the flow of electrons takes place from metal side into the semiconductor due to presence of higher energy electrons in metal. This phenomenon ends until Fermi levels of the both are perfectly aligned. This flow of electrons from metal to semiconductor causes the removal of holes from VB of semiconductor by leaving behind an unneutralized ionized acceptor (negatively charged). The extension of these negative charges takes place up to thickness W. Simultaneously, the inclusion of surface charges (positive charges having atomic separation) in metals side takes place. Finally, the establishment of electric field (from metal to semiconductor) takes place due to presence of this dipole layer of charges, this phenomenon is schematically shown in Fig. 1.22. In this case barrier height

$$q\Phi_b = \chi + E_g - q\Phi_M$$

And built-in potential $qV_{bi} = \Phi_S - \Phi_M$

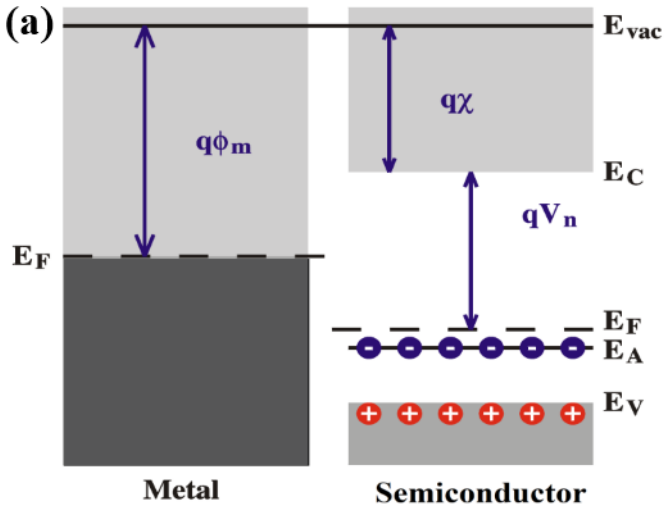

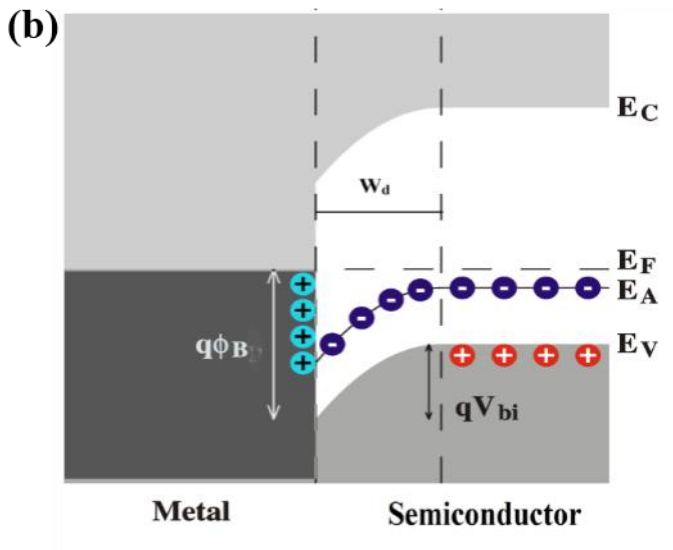

Fig. 1.22. Energy level diagram of metal and semiconductor (a) before the contact (b) after the contact [Singh (2010)]

In the thermal equilibrium, there is no current. If the biasing of the semiconductor is positive (by voltage V_F) as compared to that of metal, the decrement in the built-in potential (from qV_{bi} to $q\ (V_{bi} - V_F)$) takes place for the holes in the semiconductor. This leads to flow of more holes from semiconductor to the metal which is liable to increment in current beyond its thermal equilibrium value. Nevertheless, since $q\Phi_b$ remain almost unchanged, there is no change in the value of current (exists net flow of current) from semiconductor to metal due to no voltage drop across metal. Conversely, the reverse bias (V_R) reduces the holes flow from the semiconductor to the metal, and hence reduces the current (from semiconductor to metal) below its equilibrium value as shown in the energy band diagram (Fig.1.23). In Integrated Circuits, the external connections are always metallic. A metal-semiconductor junction, which conducts current in only one direction, may be problematic. To handle the same, there is a need to have ohmic contact, defined as a metal/semiconductor contact having a really small contact resistance in accordance with

the bulk or spreading resistance of the semiconductor. An appropriate ohmic contact shouldn't considerably trouble the device efficiency, and it may provide the mandatory current with a voltage drop that's adequately small compared to the drop over the active region of the device.

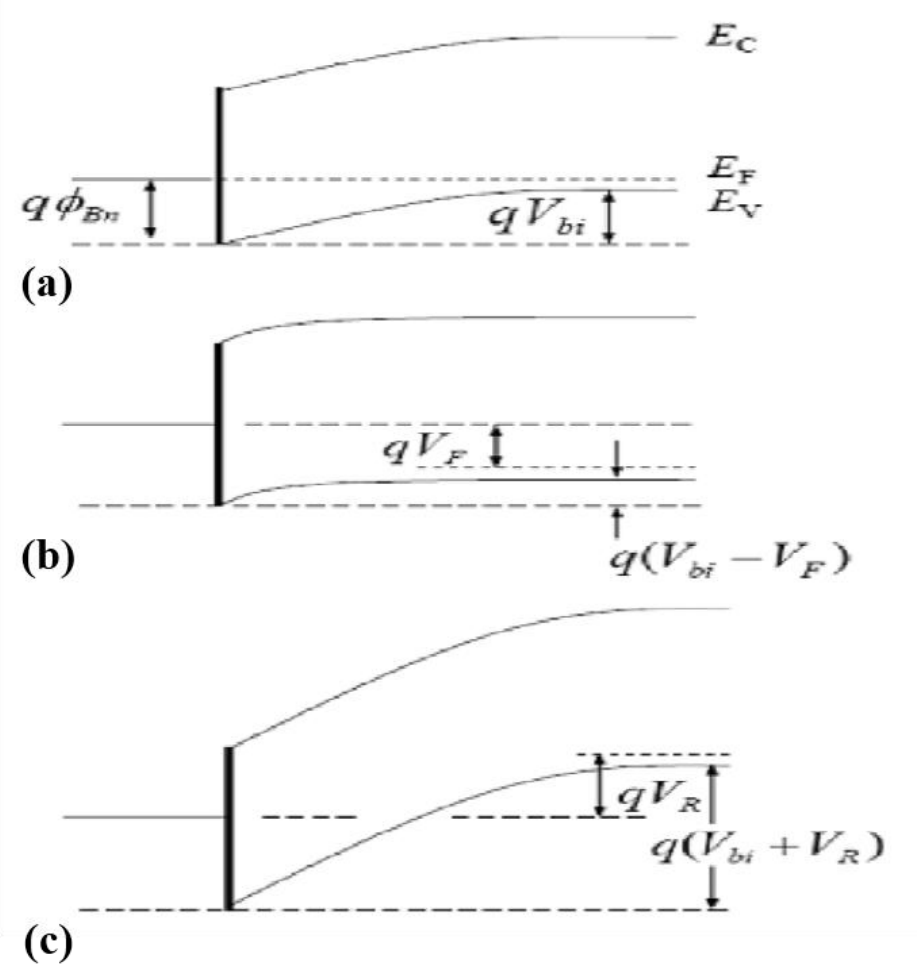

Fig. 1.23. Energy level diagram of metal/semiconductor (p-type) interface under (a) thermal equilibrium (b) forward biasing and (c) reverse biasing [Sze (1981)].

Ohmic contact

Essentially, there exists two major strategies to create the ohmic contacts. First strategy can be utilized by forming the reduced barrier height at the metal/semiconductor interface. In

such situation the current through thermionic emission process will dominate the overall transport due to lowering in the doping concentrations. The second strategy can be utilized by the increasing the doping level of semiconductor. In this case the current through the tunneling process will dominate, where the doping concentrations is strongly subjected to contact resistance.

Case 1 & 2- when $\Phi_M < \Phi_S$ for n-type semiconductor and when $\Phi_{M>} \Phi_S$ for p-type semiconductor

When a metal is in contact with a semiconductor (when $\Phi_M < \Phi_S$ for n-type semiconductor), the flow of electrons takes place from metal into semiconductor and this process ends until the Fermi levels of these two are perfectly aligned. The negative charge of electrons that accumulate in the semiconductor is confined to a thickness on the order of Debye length and essentially a surface charge. Thus there is no depletion region in the semiconductor; no barrier exists for electrons flow either from the semiconductor into metal or in the opposite direction as shown in Fig.1.24. When a bias is applied to this system, practically all the applied voltage appears across the neutral semiconductor. This type of **non-rectifying** contact is called ohmic contact.

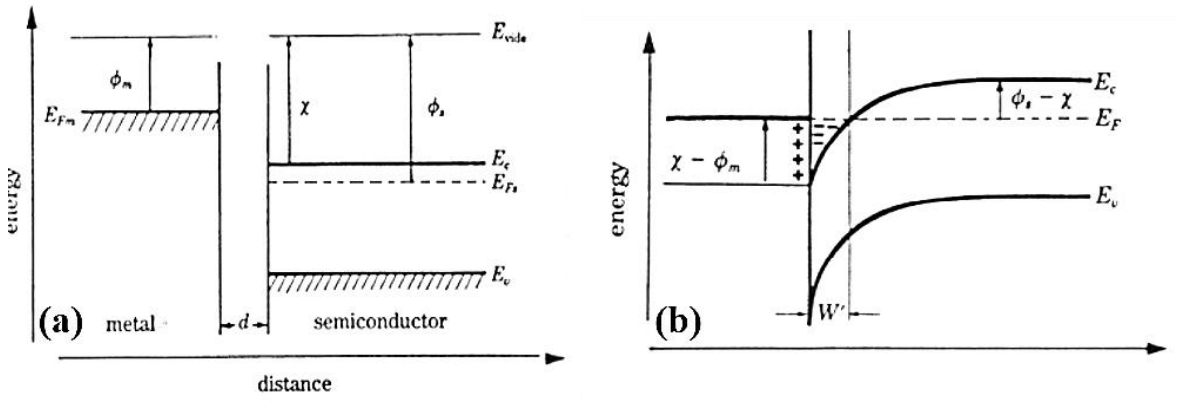

Fig.1.24. Formation of energy level diagram in metal and semiconductor (a) before the contact (b) after the contact [Streetman (2000)].

1.5.3 Current transport mechanisms in the Schottky diode

As discussed earlier, in the Schottky devices, the flow of current mainly takes place due to thermal effect or by the applied voltage. This flow of current across the metal-semiconductor junction is because of majority charge carriers. Here the same thermionic emission theory is being used to describe the transport properties of conjugated polymer-metal interfaces. This is just because the tunneling and hopping phenomenon with the help of excited phonons from the lattice vibrations is quite similar to the thermionic emission process in conventional semiconductors. There exists various charge transport mechanisms to across the Metal-Semiconductor junction. These mechanism includes (1) transportation of electrons from semiconductor (over the barrier potential) into the metal operated at room temperature (300 K) (A dominant method for Schottky diode with mildly doped semiconductors), (2) Tunneling of carrier through the barrier potential (important for heavily doped semiconductor and responsible for some ohmic contact), (3) carrier recombination and/or generation in the depletion region, and (4) carrier recombination in the neutral region, which can be comparable to minority-carrier injection (as shown in Fig. 1.25). In a perfect metal-semiconductor system, the potential energy barrier to the movement of charge carriers is mainly identified by the work-function difference involving the metal as well as the semiconductor. Generally, the barrier height directly related to the two parameters i.e., impurity concentration as well as the electric field component at interface. Hence, the recombination process in the case of Schottky has no importance as it's a majority carrier device (as stated earlier). Thus, Schottky diodes have a considerably faster response under forward bias conditions than conventional p-n junction diodes. That is why, Schottky diodes are utilized in the purposes where in actuality the speed of response matters; like, in mixers, microwave detectors, and varactors.

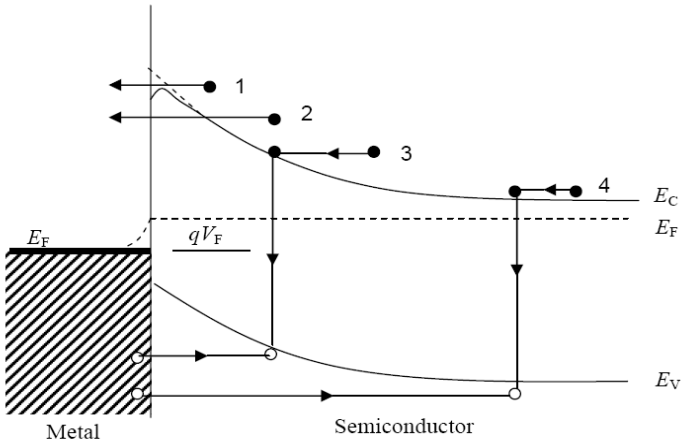

Fig1.25. Current flow mechanism in Schottky Diode [Sze (1981)].

(a) Thermionic emission current

The current transport through the device by emission over the barrier is essentially a two-step process. In the first step, the transport of electrons through the depletion region takes place, which is determined by diffusion and drift mechanism. In the second step, the electrons must undergo emission over the barrier into the metal, where the number of electrons impinging per second on the metal is the controlling factor. This is essentially known as the "thermionic emission" of current transport [Sze (1981)]. According to the diffusion theory, the distribution of the driving force takes place throughout the depletion region. With the help of analysis, the current produced through thermionic emission, may be written in the following form:

$$J = J_0\left[\exp\left(\frac{qV}{\eta kT}\right) - 1\right] \tag{1}$$

$$J_0 = A^* T^2 \exp\left(\frac{-q\phi_B}{kT}\right) \tag{2}$$

$$A^* = \frac{4\pi q m^* k^2}{h^3} \tag{3}$$

Where ***J*** denotes current density, J_0 denotes saturation current density, **m*** denotes the effective mass of electron, **q** denotes the absolute charge of electron, ***h*** denotes the Planck's constant, ***k*** denotes the Boltzmann's constant, ϕ_B is barrier height, ***T*** denotes absolute temperature, and η is ideality factor. The calculated value of the Richardson's constant (***A****) (for a free electron) is 120 $A^2/ K^2 m^2$.

(b) Current due to Quantum Mechanical Tunneling

For a heavily doped semiconductor for operation at low temperatures, the tunneling current may become the dominant transport process [Crowell et al. (1969), Padovani et al. (1966)]. Quantum-mechanical tunneling through the barrier comes into the picture and due to the wave-nature, the electrons penetrate through thin barriers.

(c) Generation-Recombination Effects

The carrier generation (across the gap) by means of thermal excitation in the case of wide-bandgap organic semiconductors (conducting polymers) is very small hence, it's generally neglected during calculations [Walker et al. (2002)]. This is especially important at reasonably reduced temperatures (175K to 235K) and a lightly doped semiconductor (i.e., large depletion width). This is similar to recombination in the p-n junction. The electrons from metal and holes from semiconductor are recombined in the depletion region. The expression for the depletion region generation-recombination current derived for the p-n junction is valid for Schottky barrier diode.

$$I_{rg} = I_{Ro}\left[e\frac{V_a}{2V_t} - 1\right] \tag{4}$$

Where the current contribution, I_{rg}, due to the generation-recombination mechanism I_{R0} is the saturation value of the generation-recombination component of the current I_{rg}.

$$I_{Ro} = \frac{pWn_i w}{2\tau_0} \tag{5}$$

where; n_i is intrinsic carrier concentration, W is depletion width, A is area of the depletion width, and τ is the effective carrier lifetime in the depletion region.

(d) Minority Carrier Injection Ratio

The Schottky diode is a majority-carrier device under low injection. At sufficiently high forward bias, the minority carrier injection ratio (ratio of minority carrier current to total current) increases with current due to the enhancement of the drift-field component, which becomes much larger than the diffusion current.

1.5.4 Extraction of device parameters from J-V and C-V characteristics of Schottky diode

The basic parameter of Schottky diode has been extracted through the current density-voltage (J-V) characteristic across its terminals. As the semiconducting polymer behaves as a lightly doped p-type material, the electrical characteristics of conducting polymer Schottky junction have been analyzed by assuming the standard emission-diffusion theory. According to this theory, the J-V relationship is expressed as

$$J = J_0\left[\exp\left(\frac{qV}{\eta kT}\right) - 1\right] \tag{1}$$

Where $J(=I/A)$ is current per unit area, J_0 the saturation current density in the absence of external bias, **q** is the electronic charge, **V** is the applied voltage, **T** is the absolute temperature, η is diode quality factor (ideality factor), and k is the Boltzmann constant. Further J_0 is related to the Schottky barrier height, ϕ_B as

$$J_0 = A^* T^2 \exp\left(\frac{-q\phi_B}{kT}\right) \tag{2}$$

Where $\mathbf{A^*}$ is the effective Richardson constant. By making use of free electron value for A^* as 120 $Acm^{-2}K^{-2}$, ϕ_B can be evaluated from J_o.

The ideality factor *n* gives a measure of the quality of the junction, which is highly process dependent. For an ideal Schottky junction, $n = 1$. In practice, however, larger values are obtained due to the presence of non-ideal effects or components to the current through the junction. However, in real Schottky contacts, an ideal behavior deviation is frequently observed and the *I–V* curves deviate from Eq. (1). The Schottky effect, series resistance, the presence of other transport mechanisms, and inhomogeneous Schottky barrier heights [Pippenger et al. (1996), Yakuphanoglu et al. (2007), Krishna et al.(2009)], have been confirmed by several authors as the most important causes of non-ideal behavior.

The mismatch in the energy position of the majority carrier band edge of the semiconductor and the metal Fermi level across the MS interface is known as Schottky barrier height. The value of barrier height ϕ_B conducting polymers based Schottky diode can be evaluated from

$$\phi_B = \frac{kT}{q}\ln\left[\frac{A^*T^2}{J_0}\right] \tag{6}$$

Considering the forward J-V characteristics for $V>kT/q$, the Eq. (2) can be approximated as

$$J = J_0 \exp\left(\frac{qV}{\eta kT}\right) \tag{7}$$

According to Eq. (7), ln(*J*) vs. V should be linear for Schottky diode configurations. The reverse saturation current was determined by the intercept of ln(*J*) vs. V at V= 0. Using the value of $J_{0,}$ the barrier height was determined from the Eq. (6).The value of the ideality factor for these devices was determined from the slope of the plot ln(*J*) vs. V at a particular temperature using Eq.(8).

$$\eta = \frac{q}{kT}\left[\frac{\partial V}{\partial \ln(J)}\right] \tag{8}$$

Further, the mobility parameter has been calculated using **Mott- Gurney's** equation in the present thesis work and explained later in details.

1.6 Requirements for Materials' engineering

The systematic advancement in materials' engineering can be duly guided by understanding the fundamentals of structural behaviors, particularly from atomic to microstructural to mesoscopic scales. By means of structural control at appropriate length scales along with knowledge of basic physical or chemical processes, it is possible to raise the engineering breakthroughs and thoughtful design of new materials. The designing of the new materials can be done either by aggregating about the polymer backbone or by incorporating the foreign conducting nanomaterials in order to improve the materials properties especially electronic properties. In either case, the motto is to enhance the conducting domians so that charge transfer can occur easily by inter-domain hoping. For example, in the case of some class of OCPs like regioregular PATs, optical and electrical properties can be significantly enhanced by understanding the control of its degree of crystallinity [Noriega et al. (2013), Scholes et al. (2017), Casalini et al. (2017), Steyrleuthner et al. (2014), Smith et al. (2017), Zhao et al. (2017)]. Thus, an ordered structure, particularly in semiconducting polymers, is of critical importance for determining as-developed device properties and its performance. Inherently, heterocyclic conducting polymers with the delocalized π-electron system has drawn much attention as active material as the semiconducting ordered film (pure or its composite form) for diodes, FETs and photovoltaic cells. This is due to excellent processability, good thermal conductivity, good air stability, and easy

functionalization capability [Lei et al. (2016), Wu et al. (2009), Kang et al. (2015)]. Apart from these, the ordered structures associated with such polymers are capable of intimate contact with adjacent polymer backbone as well as with the surface of the current collector that facilitates charge conduction [Lei et al. (2016)]. Regioregular poly (3-alkylthiophene)s, rr-P3ATs (where A is butyl, pentyl, hexyl, decyl, dodecyl etc.), poly (3,3'''-alkylquarterthiophene)s, PQT- Cη (where η=12, 14) and poly(2,5-bis(3-alkylthiophene-2-yl)thieno[3,2-b]thiophene), pBTTT-Cη (where η=12, 14, 16) are amongst the most widely studied conducting polymers. The aggregation and crystallization behavior of the polymer depends on the chemical structure of individual chains. These polymers have the capability to self-orient into a specific manner in its solution state when subjected under a given set of conditions. For example, such polymers generally consist of ordered lamellar structures in which the charge-transport typically occurs along the linear conjugated backbones (intramolecular-commonly known as J-aggregates) and through the stacked π-conjugated backbones (intermolecular-commonly known as H-aggregates) [Wu et al. (2009), Kang et al. (2015), Holliday et al. (2013)]. Here the fundamentals of structure-property correlation and various possible strategies for orientations of PATs in bulk and film formation for electronic applications are explored.

On the other hand, incorporation of conducting NPs to the polymer matrix also is also another concept in order to beautify the charge conduction properties, because nanomaterials are capable to establish proper intimacy with the polymer.

In view of above concepts, we did literature survey emphasized to earlier work done based on PATs orientation as well as incorporation of conducting additives in polymer matrix and tabulated in Table. 1.3 to 1.4. From these surveys, we concluded that most of the work

were done on orientation of RR-P3HTs into fiber form in different solvents like chloroform, toluene, xyene etc. and applied as improved electronic properties. On the other hand, incorporation of nanomaterials or nanosheets into polymer or metal oxides matrix has been utilized in numerous areas of application using CVD, hydrothermal, electro-spinning, electro-deposition, sol-gel, etc., as shown in Table 1.5 to 1.6.

Chapter 1

Table 1.3. Various applications of self-assembled PATs prepared by different techniques.

Polymers	Solvent(s) used	Technique used (Fiber preparation/Film processing)	Morphology	Application	Mobility (cm^2/Vs)	References
P3HT	Chloroform	Electro-spinning method	Fibers	OFET	$1.62x10^{-1}$	Chen et al. (2015)
P3HT	Chloroform	Solution ageing/Spin coating	Fibers	OFET	$7.0x10^{-3}$	Bielecka et al. (2011)
P3HT	Chloroform	Solution ageing/Spin casting	Fibers	OFET	0.102 ± 0.015	Kleinhenz et al. (2016)
P3HT	Chloroform/2-Methylpentane	Solution ageing/Spin casting	Fibers	OFET	~0.198	Persson et al. (2017)
P3HT	Chloroform	UV ageing/Blade casting	Fibers	OFET	0.241	Persson et al. (2017)
DF-P3HT	Toluene	FTM/FTM	Nano alignments	OFET	8.0	Nawaz et al. (2017)
P3HT	Chlorobenzene-1,2,4-trichlorobenzene	Solvent mixing/Spin casting	Nanofiber	OFET	0.012	Na et al. (2017)
NR-P3HT	Chloroform	FTM/FTM	Nano alignments	OFET	$3.4x10^{-3}$	Pandey et al. (2016)
PQT-C12	Chloroform	Solution ageing	Fibers	Diode	$1.5x10^{-3}$	Singh et al. (2017)
PQT-C12	Chloroform	FTM	Nano alignments	FET sensor	$8.77x10^{-3}$	Kumar et al. (2019)
PQT-C12	Chloroform	Solvent annealing/Spin casting	Nano alignments	FET	$3.2x1\ 0^{-3}$	Kang et al. (2014)
PQT-C12	Toluene	Roll transfer printing	-	FET	0.17	Kushida et al. (2011)
PBTTT-C14	Chloroform-toluene blend	Solution ageing	Fibers	Diode	$6.99x10^{-3}$	Singh et al. (2017)
PBTTT-C14	Chlorobenzene	FTM	Nano alignments	OFET	$8.6x10^{-3}$	Pandey et al. (2019)
PBTTT-C14	Chloroform	Spin casting	Nano alignments	OFET sensor	0.049	Sahu et al. (2017)
PBTTT-C12	1,2-dichlorobenzene	Spin casting	-	Flexible OFET	$3.1x10^{-2}$	Bae et al. (2017)

Table 1.4. Various applications of self-assembled PATs based blends and copolymers prepared by different techniques.

Polymers	Solvent(s) used	Technique used (Fiber preparation/Film processing)	Morphology	Application	Mobility (cm^2/Vs)	References
rr-P3HT-b-rs-P3HT	Anisole	Self-seeding/Spin casting	Fiber	FET	$6.3x10^{-3}$	Li et al. (2017)
P3HT-PCBM	Toluene	Solution ageing/Spin casting	Fiber	OFET	0.01	Janasz et al. (2017)
P3HT-BTTT	Chloroform	Self-seeding/Spin casting	Nano alignment	OFET	~0.044	Chu et al. (2015)
P3HT-DOBS	Chloroform	Mixing/Spin casting	Globules	OFET	$0.84x10^{-3}$	Tan et al. (2016)
P3HT-PS	1,2-Dichlorobenzene	Mixing/Spin casting	-	OFET sensor	-	Han et al. (2016)
P3HT-PS	Chloroform	Solution ageing/Shear coating	Nanowires	OFET	~0.064	Chang et al. (2016)
N-P3HT-PBTTT	Chloroform	FTM	Nano alignment	OFET	0.1	Pandey et al. (2017)
P3HT-b-PMMA	Chloroform	Solvent mixing/Spin casting	Nanofibers	-	-	Ji et al. (2017)
P3HT-PCBM	Toluene	Coating	-	CE-FET	-	Yang et al. (2017)
P3HT-PS	p-Xylene	Solvent mixing/Spin coating	Nanofibers	OFET	$7.58x10^{-3}$	Chung et al. (2019)
PQT-C12-PS	Chlorobenzene	Solvent ageing/Spin casting	Nanoalignment	OFET	~0.08	Sun et al. (2009)
PQT-C12-PS	1,2-dichlorobenzene	Spin casting	-	OFET	0.08	Lu et al. (2013)

Chapter 1

Table 1.5. Graphene/Metal Oxide nanocomposite for Gas sensor applications.

Target Gas	Sensor Materials	Synthesis Route	Conc. (ppm)	Response	References
NH_3	SnO- Graphene	CVD	50	21%	Kumar et at. (2017)
NO_2	SnO_2–graphene	sol–gel	20	9.6%	Srivastava et al. (2016)
NH_3	ZnO nanowires–rGO	thermal reduction	50	19.2%	Wang et al. (2018)
NH_3	ZnO–rGO	hydrothermal	1	24%	Singh et al. (2012)
NO_2	ZnO–rGO	solvothermal	5	25.6%	Liu et al. (2014)
NO_2	In_2O_3–rGO	hydrothermal	5	37.81%	Yang et al. (2014)
NO_2	Cu_xO–graphene	vacuum-assisted reflux	0.097	27.1%	Yang et al. (2014)
HCHO	ZnO–rGO	CVD	9	52%	Mu et al. (2014)
NH_3	Co_3O_4–rGO	electrospinning	5	53.6%	Feng et al. (2016)
NO_2	Co_3O_4–rGO	hydrothermal	60	82%	Chen et al. (2013)

Table 1.6. Various applications of hybrid material synthesised by different procedures.

Hybrid Materials	Synthesis Procedure	Application	Structure	References
TiO_2–graphene	solvothermal process	photocatalytic activity	NPs on GS	Sun et al. (2012)
	self-assembly	photocatalytic and electrochemical activity	3D hydrogel	Zhang et al. (2013)
	self-assembly	LIBs	NPs	Wang et al. (2009)
	chemical synthesis	LIBs	paper	Hu et al. (2003)
	calcination process	photocatalytic activity	graphene-encapsulated hollow nanospheres	Zhang et al. (2013)
	reduction-hydrolysis technique	photocatalytic activity	sandwich	Tu et al. (2013)
	electrostatic deposition	photoconversion properties	multilayer films	Manga et al. (2009)
VO_2–graphene	chemical synthesis	LIBs	graphene-coated NPs	Chao et al. (2015), Nethravathi et al. (2012)
	hydrothermal process	electrochemical capacitor	NPs	Deng et al. (2013)
	chemical synthesis	LIBs	ribbons	Yang et al. (2013)
MnO_2–graphene	self-assembly	supercapacitors	graphene-wrapped honeycomb NPs	Zhu et al. (2012)
	layer-by-layer assembly	LIBs	thin films	Yu et al. (2011)
Mn_3O_4–	hydrothermal process	supercapacitor	nanorods on GS	Lee et al. (2012)

Chapter 1

graphene				
	hydrothermal process	supercapacitor	NP anchored rGO	Li et al. (2013)
	hydrothermal process	carbon dioxide adsorption	porous material	Ding et al. (2012)
	hydrothermal process	LIBs	NPs	Park et al. (2014)
	hydrothermal self-assembly method	supercapacitor	3D network	Li et al. (2013)
MnO–graphene	hydrothermal process	LIBs	nanosheets	Zhang et al. (2012)
ZnO–graphene	chemical synthesis	white LEDs	quasi-QDs	Son et al. (2012)
	hydrothermal method	photocatalytic activity	nanomesh	Akhavan (2014)
	functionalisation of NPs followed by hydrothermal method	photodetector	core–shell	Shao et al. (2013)
	thermal evaporation technique	UV photodetector	NWs on 3D graphene foam	Boruah et al. (2015)
	atomic layer deposition, CVD	sensor (formaldehyde)	films	Mu et al. (2014)
	freeze-drying, subsequent heat treatment method	LIBs	NPs anchored on graphene	Li et al. (2014)
Fe_2O_3–graphene	hydrothermal process	LIBs and arsenic removal	network	Li et al. (2014)
	hydrothermal process	nonenzymatic H_2O_2 biosensors	NPs decorated on rGO	Wang et al. (2014)
	solvothermal induced self-assembly	LIBs	aerogels	Wang et al. (2014)

1.7 Motivations and research work outlines

As per earlier discussion, the charge transport property stands as the prime factor for the performance of organic electronic devices, which is strongly dependent on structural order and alignment/orientation of the semiconducting polymer chains. Similarly, the nanocomposites (organic/inorganic hybrid or graphene/ metal oxide nanostructures) can also be the alternative to achieve the enhanced charge transport properties. The controlled self-assembly in the case of organic polymers, conducting template (DNA) based assembly or nanostructures alignment (in case of inorganic metal oxides) leads to enhancement in the charge transport and ultimately in the device performance. Herein, the case of DNA templated organic polymer assembly is the consequence of better charge transport due to injection of charge by polymer into DNA. Though, all these properties are mainly depending on the nature of organic molecules and casting techniques used to form the solid polymer films over the substrates or devices. Basically, specific orientation favors the charge transport. For example GC rich DNA exhibits better charge conduction through short distance hopping but strong donor can increase this phenomenon by the injection of charge carriers (refer chapter 5 for details). After widespread literature search as summarized above we observed that there is still need to have a facile optimization for self-assembly, carrier injection assisted charge transport and further need of extensive study related to nanocomposites, over the most potential organic polymers rr-PQT-12, and rr-pBTTT-C14 of polythiophene family for electronic applications. Moreover, nanocomposites based on metal oxides or polymer matrix might be a better choice to achieve the improved charge transport properties. Therefore, the main objectives of the thesis are as follows:

- To optimize the self-assembly for organic polymers and to explore the effect of aggregation in terms of enhanced performance of Schottky devices (vertical diodes).

- To have a precise control over the molecular ordering, film morphology, arranged crystalline orientation of semiconductor domains of organic molecules and polymers during deposition.

- To study the fibril growth in the most potential organic polymers rr-PQT-12, and rr-pBTTT-C14 thin films for improvement of its property and performance of electronic devices.

- To optimize the interaction of hydrophilic GC rich DNA with hydrophobic rr-PQT-12 with the help of positively charged surfactant, and study of its junction behaviour with metal.

- To study the optoelectronic properties by incorporating conducting materials into polymers as well as fibrous metal oxides